Acknowledgement

Oslo, August 2013

Sazzad Hossen Toushik

Abstract

The structural determination of MgtB is not only necessary to reveal its unknown mechanism but also would be of great value to compare with other Mg^{2+} transporters in the Mg^{2+} transport system. Like most gram negative bacteria, *Salmonella typhimurium* also possesses MgtB transporter in Mg^{2+} transport system. The gene *mgtB* encodes the ~100.0 kDa MgtB protein that is considered a P-type ATPase. The protein sequence shows more similarity with the eukaryotic P-type ATPase family members compares to the family members of prokaryotic P-type ATPase. It is assumed that, MgtB transports Mg^{2+} across the plasma membrane to counteract reduced Mg^{2+} concentrations under growth conditions along with other transporters in Mg^{2+} transport system. The experiments that are described in this thesis were performed to characterize the Mg^{2+} transporter protein, MgtB from *S. typhimurium* by using expression, purification and crystallization techniques.

Purification was optimized of the recombinant protein MgtB; the experimental result gives an idea about the buffer, pH and salt concentrations in which MgtB was more stable. The result showed that MgtB is more stable in 10 mM Tris-HCl pH 7.6 and 100 mM NaCl concentration. It was also observed that the lipid bilayers of MgtB protein was adequately solubilized by the detergent DDM, however during purification the detergent $C_{12}E_8$ showed better analytical result. No protein crystals were observed from MgtB crystal setup in this study, even though some crystal was observed in some conditions but it turned out to be either salt or detergent. We assumed that this could have happened because of protein aggregation and instability. To avoid this problem in the future, additional experiments that include lipidation and biochemical characterization has been suggested to achieve a crystal structure of MgtB.

List of acronyms

Mgt	Magnesium transporter
KNA	Kanamycin
DNA	Deoxyribonucleic acid
His	Histidine
TEV	Tobacco Etch Virus
HKA	H^+/K^+-ATPase
NKA	Na^+/K^+-ATPase
HMA	Heavy metal ATPase
ATP	Adenosine triphosphate
SR	Sarcoplasmic Reticulum
Asp	Aspertic acid
ADP	Adenosine diphosphate
pI	Isoelectric point
kDa	Kilo Dalton
NMR	Nuclear magnetic resonance
SDS-PAGE	Sodium dodecylsulfate- polyacrylamide gel electrophoresis
DLS	Dynamic light scattering
LB	Luria Broth
RPM	Revolutions per minute
μl	Micro Liter
C	Celsius
μg	Micro Gram
ml	Milliliter
L	Liter
OD	Optimal density

IPTG	Isopropyl-β-D-1-thiogalactopyranoside
NaCl	Sodium Chloride
KCl	Potassium Chloride
PMSF	Phenyl methyl sulfonyl fluoride
BME	Beta-mercaptoethanol
HPH	High pressure homogenizer
$MgCl_2$	Magnesium Chloride
Psi	pressure per square inch
MPa	Megapascal
mM	Millimole
IMAC	Immobilized metal ion affinity chromatography
Ni	Nickel
β-DDM	β-n-dodecyl -D-maltoside
$C_{12}E_8$	Octaethylene glycol monododecyl ether
$NiSO_4$	Nickel(II) sulfate
SDS	Sodium dodecyl sulfate
DTT	Dithiothreitol
mA	Milliampere
SEC	Size exclusion chromatography
GF	Gel filtration
ddH_2O	Degassed distilled water
CMC	Critical micellar concentration
EDTA	Ethylenediaminetetraacetic acid
DOPC	1,2-dioleoyl-sn-glycero-3-phosphocholine
EtOH	Ethanol
μM	Micromole

BSA	Bovine Serum Albumin
W/V	weight/volume
V/V	volume/volume
UV	Ultra Violate
MW	Molecular weight
nm	Nanometers

CONTENTS

RESULTS

DISCUSSION

1. Introduction

1. 1 Background

Mg^{2+} is one of the foremost elements in both biological systems of prokaryotes and mammals. From the aspect of profusion, the position of Mg^{2+} within living cells is second. Due to unique chemical properties, Mg^{2+} has the largest hydrated radius, smallest ionic radius and highest charge density because it binds water molecule more tightly than other cations do [1]. The hydrated Mg^{2+} cation is 400-fold larger than the volume of the atomic ion, whereas it is only 4-30 fold large in the Na^+, K^+ or Ca^{2+} cation [2]. This biological divalent cation plays one of the vital roles in cell's structural properties; it performs the catalytic action over 300 enzymes, along with ATP utilizing or synthesizing enzymes, and binds to the specific metal site of protein to make new properties [3-6]. As a component of chrophyll molecules, Mg^{2+} has a major role in the growth of plants [1]. In many proteins, Mg^{2+} acts as both cofactor and regulator and in membranes, ribosomes and other cellular structures it functions as a regulatory and stabilizing factor [4, 5, 7-9]. Mg^{2+} transport and intracellular content are both, independent and individually more active in metabolic action [9]. It has been identified in recent studies, however does not fully explain as to how Mg^{2+} is controlled intracellularly and negotiated across membranes [6]. Nonetheless, Mg^{2+} uptake, transport and homeostasis systems in eukaryotes, mostly in mammals are weakly studied at the physiological and molecular level [1], because of limited techniques in examining Mg^{2+} [6, 9]. On the other hand, Mg^{2+} transport systems in prokaryotes have already been identified and established using highly developed genetic and molecular techniques for identifying chromosomal loci and mutations which are occupied for transport of Mg^{2+} [10]. Similar to previous studies [6], the gram-negative bacteria *Salmonella typhimurium* has been chosen as the model organism for this experiment.

1.2 Mg^{2+} transport system: MgtB protein, member of P-type ATPase in *Salmonella typhimurium*

The *Salmonella typhimurium* bacteria and mostly gram negative bacteria have three distinct Mg^{2+} transport systems, designated by *corA/mgtE, mgtA, and mgtB* [11-15]. Every transporter is encoded by its respective gene [11, 16]. MgtB is encoded by the gene, *mgtB* which is member of the family of ATPase and subfamily designated by P-type ATPase [14].

1.2.1 P-type ATPase family

P-type ATPases are a family of cations, mostly present in all species from bacteria to mammals that works as an ion pump by mediating membrane flux of all common biologically relevant cations such as Na$^+$, K$^+$, Ca^{2+}, H$^+$ and Mg^{2+}. It associates with many fundamental biological processes which range from the generation of membrane potential to completing the process of muscle contraction [17]. In the stomach, gastric H$^+$/K$^+$-ATPase (HKA) acidifies the lumen and the heavy metal ATPase (HMA) performs metal homeostasis by removing toxic ions from cells (prokaryotes and eukaryotes) and transporting specific ions in the cell membrane against a concentration gradient using ATP [17-19]. The transport mechanism of the members of P-type ATPase, including Na$^+$/K$^+$-ATPase, was discovered by the Nobel laureate Jens Christian Skou in 1957 [20]. The mechanism of P-type ATPase involves phosphorylation of a conserved aspartate on a residue in the cytoplasmic domain, by ATP and hydrolysis. This aspertyl phosphate is in an inherent feature of the P-type ATPases and subsequently is a necessary part of the transport cycle [2, 18].

1.2.2 Classes and sub-classes of P-type ATPase

After the discovery of the Na$^+$/K$^+$-ATPase by Skou in 1957, many researchers were involved in drawing up the phylogenetic tree of the P-type ATPase family and they attempted to identify the mechanism. By using sequence analysis tools, P-type ATPase family is now classified into five main classes along with some sub-classes [21]. According to sequence homology, the classes of P-type ATPase are marked numerically from Type 1 to Type 5.

1.2.2.1 Type 1-ATPase

These ion pumps belong to one of the earliest and simplest members of the P-type ATPase family. It has two sub-classes marked as type 1A and type 1B ATPase.

1.2.2.1.1 Type 1A-ATPase: As a small class, only few bacterial ion pumps are member of this subclass along with *Escherichia coli* Kdp K^+-pump complex which has four different membrane proteins such as KdpA, KdpB, KdpC and KdpF [17]. KdpB has a molecular weight of 72kDa and is the largest subunit of Kdp [22] that contains the catalytic core and ion translocation site. As a smallest subunit of P-type ATPase, KdpB contains only six predicted membrane-spanning helices [17]. KdpA is hydrophobic with ten predicted membrane-spanning helices whereas KdpC has only one membrane-spanning helix [22].

1.2.2.1.2 Type 1B-ATPase: This subclass is involved in the transport of some soft transition-metal ions, though most of the P-type ATPases translocate small and hard cations like H^+, Na^+, K^+, Ca^{2+} and Mg^{2+}. Some proteins such as CopA, ZntA and CadA, are involved in bacterial metal resistance are included with this subclass. They are in thought to remove toxic ions like Cu^+, Ag^+, Zn^{2+}, Cd^{2+} or Pb^{2+} from cell [17]. Type 1B-ATPases work as single chain proteins and have eight membrane-spanning helices but in consensus sequence, they lack the last four helices. Interestingly, for metal recognition they have two or three additional transmembrane helices which have been found at the N-terminal side of the core domain [17, 19].

1.2.2.2 Type 2-ATPase

Among the classes of P-type ATPase, the most diverse class is Type 2-ATPase. Most of the electrogenic ATPases are considered as member of this class [17]. It has four sub-classes, marked as Type 2A-ATPase, Type 2B-Atpase, Type 2C-ATPase and Type 2D-ATPase.

1.2.2.2.1 Type 2A-ATPase and Type 2B-ATPase: Though both transport Ca^{2+} ion, Sarco (endo) plasmic Reticulum (SR) Ca^{2+}-ATPase or SERCA 1 which helps to transfer Ca^{2+} ion from the cytosol of the cell to the lumen of the SR during muscle relaxation, is comprised of Type 2A-ATPase. On the other hand, plasma-membrane Ca^{2+} pumps are included with sub-class Type 2B-ATPase. After experimental determination of the atomic structure of SR Ca^{2+}-ATPase, it has been published that SR Ca^{2+}-ATPase is the prototype of P-type ATPase which

have five additional α-helices [17, 19]. Type 2B- Ca^{2+} ATPases have essential function in regulation of plant cells. In animal cells, Type 2B-ATPase has calmodulin-binding regulatory domains in carboxy or amino terminal, whereas the activity of Type 2A-ATPase pump is regulated by phospholamban [17].

1.2.2.2.2 Type 2C-ATPase: The closely related Na^+/K^+-ATPase (NKA) and the gastric H^+/K^+-ATPase (HKA) from animal cells comprised of sub-class Type 2C-ATPase. In humans, Na^+/K^+-ATPase (NKA) targets the digitalis glycosides and used in the treatment of heart conditions. The gastric H^+/K^+-ATPase (HKA) act as a target for drugs to help reduce excess production of stomach acid in order to prevent ulcers [17]. Type 2C-ATPases are hetero-oligomers where the catalytic transport subunit referred to as α-subunit, is linked with additional subunits referred to as β and γ subunits that are also member of this sub-class [19].

1.2.2.2.3 Type 2D-ATPase: A small number of eukaryotes such as fungal Na^+-ATPases are included in this sub-class whereas most of its functions are unknown [17].

1.2.2.3 Type 3-ATPase

It is one of the most important classes of P-type ATPase that can create and maintain the membrane potential in plant and bacterial cells, that helps develop various concentrations across membranes [17]. This class has 2 sub-classes including Type 3A and Type 3B-ATPase.

1.2.2.3.1 Type 3A-ATPase: In this sub-class, H^+-pumps are exclusively part of plasma membranes that are found mostly in plants and fungi, with the exception of H^+-pumps in *Methanocaldococcus jannaschii*. H^+-ATPase has an extension at the end of both N-terminal and C-terminal. The extension of the N-terminal functions as a pH sensor to maintain an intracellular pH of ~6.6 against an extracellular pH of 3.5 [17, 19]. On the other hand, the extension of the C-terminal has auto-inhibitory function and can be released by phosphorylation or at the time of binding to regulating factors [19].

1.2.2.3.2 Type 3B-ATPase: It is a small sub-class where only three bacterial Mg^{2+}-pumps are included and has close similarity with Type 3A-ATPase [17].

1.2.2.4 Type 4 and 5-ATPase

These two classes have close similarity with class 1-ATPases. Type 4-ATPases has been found only in eukaryotes. They are involved in the transport of phospholipids [23] and maintaining the asymmetry of the lipid-bilayer [17]. It is thought that these Mg^{2+}-ATPases, which are lipid flippases, translocate as phospholipids from the outer to inner membrane of the cells such as red blood cells [17]. Type 5-ATPase has recently been identified as a new class in the eukaryotic genome but their substrate specificity and biological function is still not known. Like the members of class 1-ATPase, the N-terminal often has additional helices [19] but it is assumed that the members of this class also work as ion pumps[17].
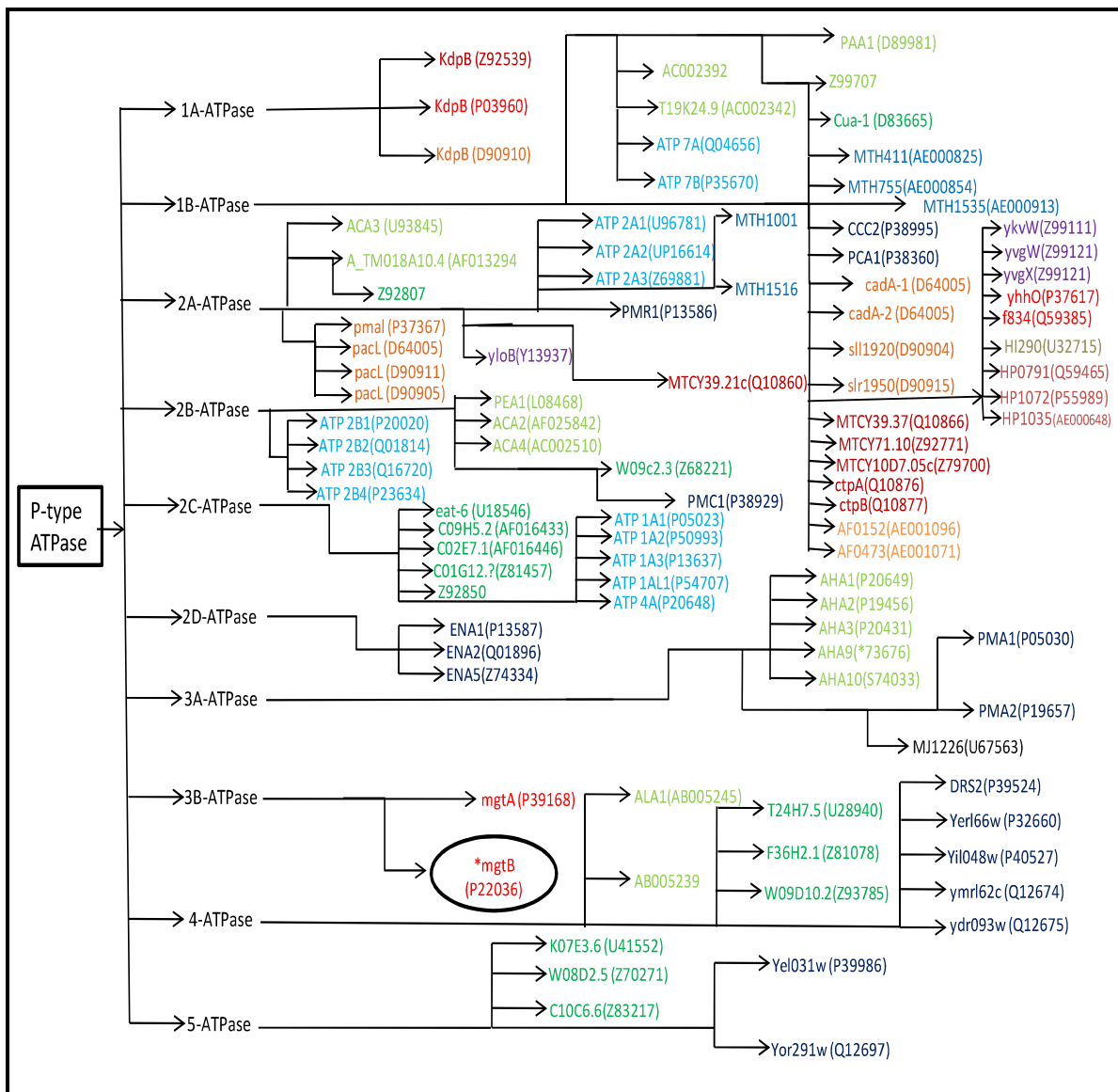
Figure 1.1: Phylogenetic tree of the P-type-ATPase family. Data collected from P-type ATPase DATABASE, maintained by Kristian Axelsen, DK. Subfamilies are classified on their ion specificities: type 1A represents bacterial Kdp-like K^+-ATPases, type 1B involves to transport soft transition-metal ions, type 2A sarcoplasmic-reticulum (SR) Ca^{2+}-ATPases, type 2B plasma-membrane Ca^{2+}-ATPases, type 2C Na^+/K^+ and H^+/K^+-ATPases, type 2D eukaryotic Na^+-ATPases, type 3A involves H^+-ATPases, type 3B for bacterial Mg^{2+}-ATPases, type 4 for lipid flippases and type 5 involves unknown substrate specificities of eukaryotic P-type ATPases. Representative gene of every species has same color coded in every subclass; Light red color for *Mycobacterium tuberculosis*, red for *Escherichia coli*, light orange for *Synechocystis* PCC6803, yellow for *Archaeoglobus fulgidus*, light green for *Arabidopsis thaliana*, green for *Caenorhabditis elegans*, light blue for *Homo sapiens*, blue for *Methanobacterium theroautotrophicum*, deep blue for *Saccharomyces cerevisiae*, purple for *Bacillus subtilis*, grey for *Haemophilius influenzae*, light pink for *Helicobacter pylori*, black for *Methanococcus jannaschii*.

1.3 Domain Structure of P-type ATPase

Though it is difficult to define the domain in a formal definition, we define the domain as a compact subunit that contains an individual polypeptide chain in a protein structure. The discovery and determination of the crystal structure of the first P-type ATPase the Ca^{2+}-ATPase SERCA1a from rabbit fast twist muscle and later the Na^+/K^+-ATPase and H^+-ATPase in the plasma membrane, has led to the establishment of the general 3D structure of P-type ATPases. Structurally, P-type ATPase has an elongated form, where its length is three times its width. Its one end placed in membrane whereas other end forms a large cytoplasmic headpiece. To form the cytoplasmic domains, the two large cytoplasmic loops attach to the end of the N and C terminal [24]. In P-type ATPases there are five individual structural and functional domains, where three are cytoplasmic and two are membrane-embedded domains. The three cytoplasmic domains are Actuator (A domain), Nucleotide binding (N domain) and Phosphorylation (P domain).Other two membrane-embedded domains (M-domain) are Transport (T domain) and Class specific support domain (S domain). Sometimes one extra domain named Regulatory domain (R domain) can be present with either N or C terminus or both in the sequence [17, 24]. In molecular mechanism of P-type ATPases, by the help of N-domain the Aspertic acid

containing P-domain is phosphorylated and reversely dephosphorylated by the A-domain [24, 25]. Five types of domains are described below.

1.3.1 A-domain

The amino terminal A-domain is a built-in protein phosphatase and has a highly conserved sequence motif TGE (Thr-Gly-Glu). This domain acts as a protein phosphatase and during ion-pumping cycle it contacts the phosphorylation site closely, as indicated by the cleavage of the TGE loop. This domain is also called the Actuator domain [17, 24].

1.3.2 P-domain

The invariant aspartic acid is transiently phosphorylated in this domain and acts as a catalytic core of the P-type ATPase family. In the middle of this domain the phosphorylation site is located with the Rossmann fold, which has two halves that are structurally similar and each consisting of two α- helix and three β-strands. Among all domains in P-type ATPases, P-domain is mostly conserved. The conserved sequence motif is DKTG (Asp-Lys-Thr-Gly) where Asp is located along with TGDN (Thr-Gly-Asp-Asn) and GDGXND (Gly-Asp-Gly-x-Asn-Asp) sequence motif .These two sequence motifs are involved in coordination of ATP binding Mg^{2+} in phosphorylation site [17, 24]. This domain also named as Phosphorylation domain.

1.3.3 N-domain

In a function of ATPase, the hydrolysis or stimulatory effects of ATP molecules are dependent on its accurate position. Since the core structure of N-domain has conserved pocket where the ATP bind and the reactive Asp residue is phosphorylated in P-domain. Here it acts as a built-in protein kinase [19, 24]. This domain has large insertions and deletions in P-domain which is also connected with two antiparallel peptide strands. This domain is the most variable among all three cytoplasmic domains. This domain is also called the Nucleotide Binding domain [17, 24].

1.3.4 M-domain

The P-type ATPase has two membrane-embedded domains (M-domain) including the Transport domain (T-domain) and Support domain (S-domain). They consist of 10 membrane

spanning segments and surrounded by the ion-binding sites in the membrane. The first 6 membrane spanning helices (M1-M6) make the formation of the transport domain (T-domain) that can move during the catalytic cycle because it is highly flexible and it can associate and dissociate the ions in time of cycle. All the domains, including A, N and P-domains, are connected with the T-domain membrane spanning helices via connecting loops. The other 4 membrane spanning helices (M7-M10) make the formation of class specific support domain (S-domain). This domain works as an auxiliary unit which gives the structural support of T-domain. In some P-type ATPases this domain helps to attach more ions in additional ion binding sites in the membrane during cycle. But this domain does not have the flexibility of the T-domain. This domain is connected with T-domain by a short connection loop and also has a connecting loop with the outer membrane. Among the various P-type ATPase subfamilies this domain has little conserved sequence [17, 24].

1.3.5 R-domain

This domain may be present in any one of the terminal ends of P-typeATPases. Many heavy metal pumps and plant calmodulin binding Ca^{2+} pumps contain R-domain in their N terminal. On the other hand, some Na^+/K^+-ATPase and animal calmodulin binding pumps contain this domain in C terminal and plasma membrane H^+ pumps contain R-domain in its both terminal. In catalytic cycle this domain acts as an auto-inhibitor when it interacts with other molecules of the pump [24, 26].
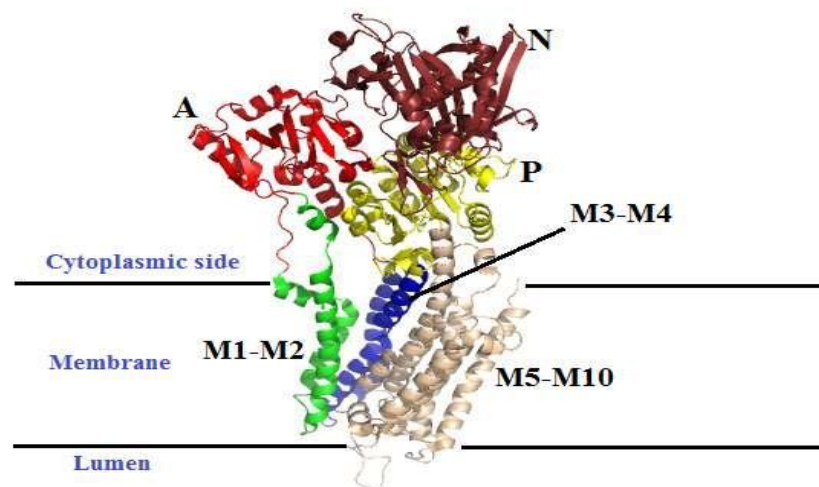
Figure 1.2: Different domains in cartoon model of the crystal structure of Calcium pump bound with ADP and TG in SERCA 1 (PDB accession number: 3AR3). In picture, domain A is marked by red color, domain N is ruby color, domain P is yellow color, transmembrane helixes M1-M2 is in green color, M3-M4 is blue color and M5-M10 is in wheat color.

1.4 Molecular Mechanism of P-type ATPase

In the translocation mechanism, the cytoplasmic and membrane domains have different roles which are essentially the same in all P-type ATPases such as ATP binding, phosphoryl transfer and hydrolysis, and in ion binding sites where the energy is released by the mechanical transduction [17]. A transporter always tries to prevent the formation of an open passage across the membranes, which is necessary to transport cations against an electrochemical gradient. However because of the problem of rapid-back flow of ions, any kind of charge or concentration gradient may be destroyed in the entire membrane. To solve this problem, in 1966 Oleg Jardetzky proposed a model named "Alternating-access model" in the function of P-type ATPases. According to this model, the access pathways closed at both sides of the membrane. For this reason, the ions are being obstructed during times of transportation before each side of the membrane opens in an alternating manner. By conformational change, the ion pumps transport ions across membranes by the influence of ATP hydrolysis. This mechanism was described by one cycle named "Post-Albers Cycle" which was proposed by Albers in 1967 and Post et.al., in 1969 [19, 27]. According to this cycle, the membrane has two states, E1 state and E2 state where the ATPase transports in an alternating manner. Ions come from the cell interior and bind to the high affinity area in the membrane domain (M-domain) of E1 state. This ion binding promotes the autophosphorylation of phosphorylation domain (P-domain), the ATP converts to ADP and the ion transfers to the phosphorylated state called E1-P state. By the help of nucleotide binding domain (N-domain), the Mg-ATP tries to make phosphorylated the phosphorylation domain (P-domain) containing Aspartic acid (Asp) residues. Nevertheless Asp residues are phosphorylated however are able to transfer the phosphoryl group which helps it to return to ADP. By conformational change, E1-P state disposed the ADP to the lower energy E2-P state. After transition of E1 to E2, the phosphorylation domain (P-domain) tries to regenerate. At the same time the actuator domain (A-domain) containing TGE loop tries to attach to the phosphorylation site which helps the phosphoryl group be protected from hydrolysis and dissociation of ADP. Here, the ADP again converts to ATP by auto-

dephosphorylation and in the middle of the transport domain (T-domain) the transported ion binds and alternates from E2-P state to E2 state. At last, the ions translocate from the lower energy E2 state to higher energy E1 state by conformational change and are exposed in extracytoplasmic side and the cytoplasmic side. During ion transportation, the net charges of ions are always being changed and moving across the membrane, that having some effect on membrane potential which depends on the direction of charge movement [17, 19, 24, 27].
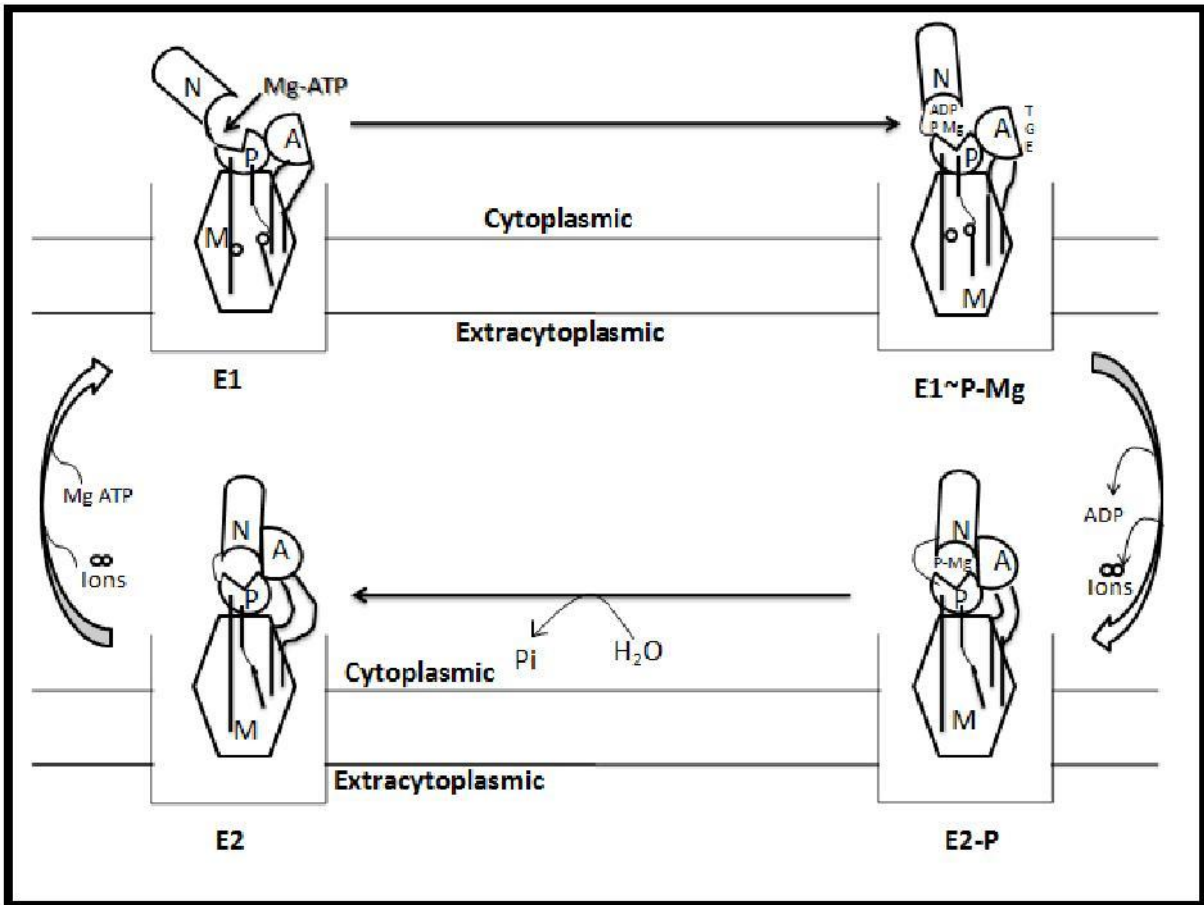

Figure 1.3: Schematic overview of the catalytic cycle of P-type ATPases. This figure is redrawn from Werner Kühlbrandt (2004).

1.5 The sequence and Putative structure analysis of MgtB: Comparison of MgtB with other P-type ATPases

The integral membrane protein MgtB, contains multiple hydrophobic regions which helps membrane spinning [14]. Although, MgtB in *S. typhimurium* is a 100.60 kDa protein and also the member of the super family of P-type ATPase, apparently it uses ATP to move Mg^{2+} with, rather than against, its electrochemical gradient, making it different from the other members of this family. By amino acid sequence analysis of MgtB and other members of P-type ATPase family, it has been revealed that MgtB is significantly less similar to other prokaryotic P-type ATPase family members (10-30% identity) but more similar to members of the eukaryotic P-type ATPase and showed 50% overall sequence identity with the sarcoplasmic reticulum Ca^{2+} - ATPase [2, 18, 28]. It also showed the similar result by hydropathy plots analysis [18].

In the P-type ATPase family, most of the amino acid length of prokaryotic P-type ATPase is on average 583 to 727, whereas the length of amino acid sequence of MgtB is 908. The molecular mass of most of the prokaryotic P-type ATPase is on average 63 to 78 kDa where as the molecular mass of MgtB is 100.60 kDa. On the other hand, the amino acid sequence length of MgtB is more similar to the eukaryotic P-type ATPase which has an average amino acid sequence length of 900-1000 [14]. In 1988, Ramon Serrano published a paper defining the 10 regions of P-type ATPases and showed the homology across all known family members [14, 29]. He concluded in his paper that MgtB is dissimilar with prokaryotic P-type ATPases and similar to eukaryotic P-type ATPases [29].

Another analysis of various P-type ATPases was done by the experimental method named Hydropathy plots. This was based on a computer program which considered the hydrophilicity and hydrophobocity of a protein with its sequence of amino acids [30]. After analysis of hydropathy plots between MgtB and various members of P-type ATPase, it was revealed that KdpB protein from *Escherichia coli* was smaller than MgtB protein from *S. typhimurium*. KdpB protein contains only two or three transmembrane loops out of four to six loops in C terminal, whereas MgtB protein contains additional transmembrane loops which make it different to other known prokaryotic P-type ATPases. Serrano and co workers was proposed that the yeast plasma membrane H^+-ATPases contain 8 transmembrane segments in their model whereas MacLennan and his group proposed 10 segments in their model for rabbit sarcoplasmic reticulum Ca^{2+}-ATPase which is proved by the hydropathy plots of MgtB because it has 10 transmembrane segments [14].

In same species (i.e. *S. typhimurium*) the protein sequence similarity between two transporters like MgtA and MgtB is significantly higher than the sequence similarity between CorA and MgtB. Sequence similarity between MgtA and MgtB is about 49% amino acid identity with additional 25% conserved amino acid substitutions. In comparison the protein sequence similarity between CorA and MgtB is about 12% according to the online Multiple Sequence Alignment program CLUSTALW. Though MgtA and MgtB proteins in *S. typhimurium* are siblings of Mg^{2+} transport P-type ATPase, surprisingly the percentage of similarity of MgtA between two species like *S. typhimurium* and *E. coli* is higher than the similarity between MgtA and MgtB in *S. typhimurium* [9].

1.6 Role of MgtB protein along with other transporters

In *Salmonella typhimurium* CorA, MgtA and MgtB, all three transporters are involved in the Mg^{2+} transportation system but under in different growth conditions. Both MgtA and MgtB transport systems may be acting as Mg^{2+} scavengers during times of Mg^{2+} deprivation in specific growth conditions. They also transport adequate Mg^{2+} to regulate growth where as the CorA transport system transports major Mg^{2+} under all growth conditions [9, 14]. Both the MgtA and MgtB transport system mediate the only influx of both Mg^{2+} and Ni^{2+} whereas the CorA transport system mediate both influx and efflux of Mg^{2+}. Even at high extracellular Mg^{2+} concentrations, the MgtA and/or MgtB transport system cannot efflux the Mg^{2+} without CorA transport system in different growth conditions. In *S. typhimurium* the efflux of Mg^{2+} occurs via four distinct chromosomal loci *corA, corB, corC* and *corD* that act as sole transporters [2, 6, 14]. *S. typhimurium* contains the PhoPQ two-component signal transduction systems which help to regulate the transcription at the time of Mg^{2+} deprivation within the growth conditions of bacteria [31]. Besides this PhoPQ is responsible for the virulence factor of *S. typhimurium* because both loci *mgtA* and *mgtCB* are regulated by these two component systems [2, 32]. During time of reduced extra cellular Mg^{2+} concentration, the transcription of *mgtCB* operon helps to dissociate Mg^{2+} from PhoQ and in turn it activates the transcription factor PhoP. The chromosomal loci *mgtCB* encodes two proteins MgtC and MgtB where MgtC protein is responsible for the virulence in mice. Recently it has been published that MgtC protein is necessary for the survival of the bacteria inside macrophages in low Mg^{2+} concentration [33, 34] that was previously unknown [6, 9, 32]. MgtB protein transport Mg^{2+} from the periplasm to

the cytoplasm to overcome the deficiency of Mg^{2+} but has no apparent role within virulence factors [33].

1.7 Growing protein crystals

Protein crystals are three dimensional arrays of protein molecules that are necessary to measure the diffraction from its signal. In late 1950s, J.C. Kendrew, M.F. Perutz and coworkers were the first to determine the three dimensional structure of myoglobin and haemoglobin by using X-ray crystallography. Before developing the method of nuclear magnetic resonance (NMR) spectroscropy in 1980s by K. Wuthrich, R.R. Ernst and coworkers, X-crystallography and fiber diffraction were the only tool available to define the macromolecular structure [35, 36]. To get a good result, it is necessary for the internal order of protein crystal to have a good pattern of molecules which will be diffracted to high resolution in time of X-ray. As a result, the good crystal will yield a highly output data and gives a detailed structure. Within its structure, the X-rays are diffracted by the electrons and create a 3-dimensional map by the distribution of electrons in the structure. Before starting the crystallization of the protein, it is important to check its activity and their biological function in order to prepare it in the proper way because proteins can unfold, be impure, insoluble or unstable. Another crucial step to consider in protein crystallography is that protein should be pure before crystallization because it is necessary for continuous and homogenous lattice growth of crystals. Nowadays many modern recombinant techniques have been established to purify the massive production of proteins with different purification-tags. It is possible to get 95% purified protein by using simple metal-based elution step in metal affinity chromatography. Another purification technique, size exclusion chromatography (SEC) has also been used to obtain homogeneous pure protein solution as a second step of purification after metal-based affinity chromatography in laboratory. To check the purity and later concentration of protein, a simple assay is being used called sodium dodecylsulfate-polyacrylamide gel electrophoresis (SDS-PAGE). For staining the gel, coomassie blue or silver staining solution is used rapidly to detect the single band of pure protein and minute amount of other impurities. Another technique that can also be used to check the homogeneity of protein solution includes the dynamic light scattering (DLS) method which measures the polydispersity of the protein sample [37]. Sometimes good crystals of pure protein also grow with derivatives like nonprotein components, which make crystals of the protein in a complex. In this reason, crystallographers need to find out the cofactors, substrate

analogs, inhibitors and allosteric effectors like ligands with in the complexes of protein structure. Protein-ligand interaction revealed by determining the full structure and is able to provide a description of the function in details. Some heavy-metal complexes called heavy-atom derivatives with crystals of protein might be necessary to solve the phase problem. In modern method, the methionine in amino acid residues of protein is replaced by selenomethionine to overcome the phase problem in protein crystallography [36].

1.7.1 Techniques of growing crystals

In general, crystal formation occurs in two steps. In the first step, nucleation occurs followed by crystal growth. Initial formation of molecular clusters in growing crystal is called nucleation which helps crystal growth. Proteins are usually denatured by heat or unfold in organic solvents. The most common method is that purified protein is dissolved in an aqueous buffer containing precipitant to precipitate the protein. In protein purification, the most common buffer containing precipitants are ammonium sulfate and polyethylene glycol. By controlling the evaporation process, water is removed from the mixture of solution and as a result, precipitation is found in the bottom of the crystal plate. To grow good and large crystals, slow precipitation is more convenient than rapid precipitation because it may produce nebulous solids or bad and small crystals.

In crystallization the two most commonly used methods are techniques of vapor diffusion where the protein solution or precipitant is allowed to equilibrate in a closed place. The closed place contains a large volume of aqueous buffer where the concentration of precipitant is optimal to grow crystals. The two common methods in vapor diffusion are hanging-drop technique and sitting-drop technique. In both techniques, the crystallization plate reservoir contains larger volumes of buffer containing precipitant than the mixture of concentrated purified protein and the same precipitant in a droplet that is hanging on the cover slip or sitting on the top of each well contained pedestal. The cover slip is sealed onto the top of each well with grease or silicon oil. As the top of each well is sealed, the vapor diffusion, like evaporation and condensation, occur in a closed system. As a result, the water is transferred from the protein solution of droplet to the reservoir until equilibration in concentration of precipitant is reached in both solutions. The concentration of precipitant within the protein solution will reach the required for the nucleation and equilibrium process to be stopped in between protein solution

and reservoir because of the inherent vapor pressure. This is equal to the close system vapor pressure [38].
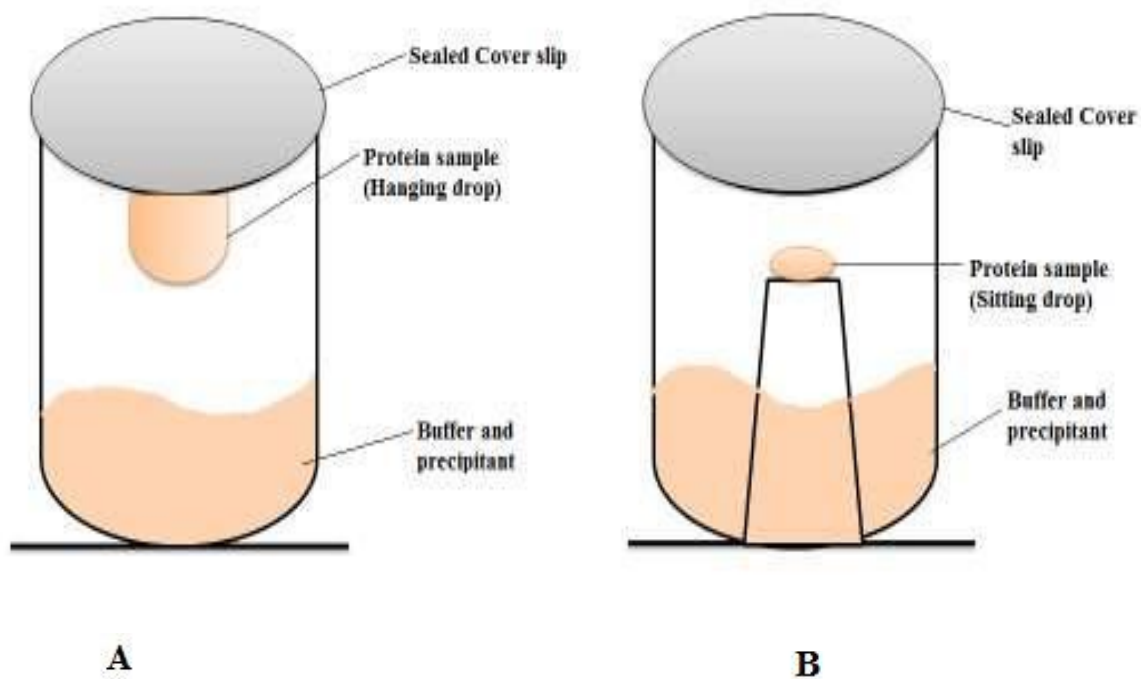
Figure 1.4: Growing crystals by two common methods; (A) Hanging-drop method, (B) Sitting-drop method.

2. Materials

2.1 Laboratory instruments

Laboratory instruments	Supplier
Multitron 2 (Shaking incubator)	InFors HT
Heraeus (Incubator)	Thermo Scientific
LEX 48-High Throughput Bioreactor	Harbinger's LEX system
Centrifuge rotor JLA 8.1000	Beckman
Centrifuge rotor JA 25.50	Beckman Coulter
Ultracentrifuge rotor 45Ti	Beckman Coulter
Ultracentrifuge rotor MLA 130	Beckman Coulter
Centrifuge rotor Sx4250	Beckman Coulter
High pressure homogenizer (HPH)	Avestin C3
Positive displacement pipette	
NanoDrop^{TM} 2000/2000c spectrophotometer	Thermo Scientific
Ni-NTA chelating HP column	GE Healthcare
Mini-PROTEAN Tetra System (Gel Electrophoresis)	Bio-Rad
ChemiDoc XRS $^+$ Imaging system	Bio-Rad
MilliQ (Q-POD)	Millipore
ELIX (E-POD)	Millipore
AKTA purifier	ÄKTA
Agilent HPLC Affinity 1260	Agilent Technologies
Vivaspin Columns	GE Healthcare
Vortex-machine	IKA
Biorupto NextGen (Ultrasonicator)	Diagenode

See-saw rockers-SSL4 (Shaking Table)	Stuart
Oven	Temptech
Leica M205 C (Stereo microscope)	Leica Microsystems
Crystallization plates (Hanging drop and Sitting drop)	
Cover slips	
Automatic Pipettes	Thermo Scientific
Pipette Tips	Molecular BioProducts
Various glass equipment's	
Ultracentrifuge tubes	Beckman specifications

2.2 Chemicals

Chemicals name	Supplier	Cat no.
1,2-dioleoyl-sn-glycero-3-phosphocholine (DOPC)	Avanti Polar Lipids	770375
2 Mercapto EtOH (BME)	Sigma-Aldrich	M7522
38% Acrylamide/ Bis solution	Bio-Rad	161-0156
DL-Dithiothreitol (DTT)	Sigma	646563
L-Ascorbic acid	Sigma	A5960
n-Dodecyl beta-D-maltoside (DDM)	Affymetrix	D3105
Acetic acid	Sigma-Aldrich	320099
Adenosine 5′ - triphosphate (ATP)	Sigma	A3377
Agar No 1	Oxoid LTD	LP0011
Bio-Beads SM-2 adsorbent	Bio-Rad	152-3920
Bovine Serum Albumin (BSA)	Sigma	A7030
Bromophenol Blue	Fisher Scientific	BP115
Coomassie Brilliant blue	Serva	17525

DNase1	Sigma	DN25
Ethylenediaminetetraacetic acid (EDTA)	Sigma	E5134
Ethanol (96%)	Sigma-Aldrich	3221
Glycerol (99.5%)	VWR International	24388.295
Hydrocloric Acid (HCl)	Sigma	H1758
Imidazole	Sigma-Aldrich	56750
Isopropyl-β-D-1-thiogalactopyranoside (IPTG)	Biogynth	I-8000
Kanamycin	Sigma	K-4000
Magnesium Chloride hexahydrate ($MgCl_2.6H_2O$)	Sigma-Aldrich	M9272
Methanol	Sigma-Aldrich	32213N
Phenyl methyl sulfonyl fluoride (PMSF)	Nigu Bioselect	140000349
Potassium Chloride (KCl)	Sigma-Aldrich	SZBA2360V
Sodium dodecyl sulfate (SDS)	Sigma-Aldrich	L4509
Sodium Chloride (NaCl)	Sigma-Aldrich	S7653
Tetramethylethylenediamine (TEMED)	Fisher Scientific	T/P190/04
Tryptone	Oxoid LTD	LP0042
Trizma base	Sigma	T6066
Triton X-100	Fisher Bio-Reagents	BP151
Tri-sodium citrate dehydrate	Merck	1.06448.0500
Octaethylene glycol monododecyl ether ($C_{12}E_8$)	Nikko chemicals	BL-8SY
Yeast Extract	Oxoid LTD	LP0021

2.3 Composotion of LB Agar media

Tryptone

Yeast Extract

NaCl

Agar No 1

ddH$_2$O

2.4 Composition of Loading Buffer (5x SDS buffer)

10% SDS

10mM DTT

20% Glycerol

0.2M Tris-HCl pH 6.8

0.05% Bromophenol blue

2.5 12% SDS-gel Preparation (2 Bio-Rad protein gels)

Separation gel

30% Acryl-bis-3.7 ml

3 M Tris-Cl pH 8.8-1.2 ml

10% SDS-91.7 µl

ddH$_2$O-3.4 ml

10%APS-91.7 µl

TEMED-3.7 µl

Stacking gel

30% Acryl-bis-0.96 ml

0,5 M Tris-Cl pH 6.8-1.4 ml

10% SDS-58.5 µl

ddH$_2$O-3.3 ml

10%APS-58.5 µl

TEMED-5.8 µl

2.6 Crystallization Screens

- ➢ MemGold^{TM}, MD 1-39, Box 1 of 2 (Molecular Dimension Limited)
- ➢ MemGold^{TM}, MD 1-39, Box 2 of 2 (Molecular Dimension Limited)
- ➢ MemSys^{TM}, MD 1-25 (Molecular Dimension Limited)

3. Methods

3.1 Expression of protein

Cloning was performed by **Kim Langmach Hein** (NCMM) using molecular biology methods. Template DNA of the Mg^{2+} transporter protein MgtB from *Salmonella typhimurium* encodes the gene mgtB was cloned into a pETM-11 vector (developed at EMBL by Gunther Stier) with 6x polyhistidine tag (His-tag) and Tobacco Etch Virus (TEV) protease cleavage site in N-terminal fusion. The pETM-11 vector with the *mgtB* gene was transformed into chemically competent *Escherichia coli* C43 (DE3) cells grown in Luria Broth (LB) medium.

3.1.1 Transformation of plasmid in cells

The process of plasmid transformation was performed by a heat-shock procedure. 1 µl of pETM-11 with *mgtB* construct was added to 500 µl of chemically competent C43 (DE3) cells and kept it on ice for 10 minutes. The heat-shock procedure was done in hot water bath (Sonication bath) at 42 °C. The cells were placed in sonication bath for 45 seconds and immediately placed on ice for ~2 minutes. 250 µl of LB medium was added to the cells under laminar air hood and was incubated in the shaking incubator (Multitron 2 from InFors HT) at 37 °C at 200 rpm for 1 hour. After incubation, cells were plated on agar plates with 50 µg/ml Kanamycin and incubated at 37 °C overnight in an incubator. A single coloni was used to inoculate a starter culture the following day.

3.1.2 Over expression of recombinant protein

The 10 ml starter culture was incubated at 37 °C overnight and then diluted to 1x Kanamycin containing 500 ml LB medium flask and incubated in a shaking incubator at 37 °C overnight. For medium scale over expression experiments, 10 ml pre-culture was diluted with 1.5 L fresh culture with 1 ml/L Kanamycin antibiotics. The fresh culture grew at 37 °C by using LEX 48-High Throughput Bioreactor System (Harbinger's LEX system) until the OD_{600} or optical density reached between 0.6 and 0.8. To induce the protein expression in the cells, 0.5 mM Isopropyl-β-D-1-thiogalactopyranoside (IPTG) was added and after reduceing the growing temperature to 21 °C, the expression experiment was performed overnight. The overnight media was harvested by centrifugation. Centrifugation was done by using the rotor type JLA 8.1000 at 7,000 rpm in 4 °C for 15 minutes. Supernatant was discarded and cell pellets were

washed by cell washing solution (50 mM Tris-HCl pH 7.6, 20 mM KCl and 1 mM PMSF). An additional centrifugation was performed in 7,000 rpm at 4 °C for 15 minutes and the supernatant was discarded after centrifugation. Over expressed cells were collected and kept in the freezer.

3.1.3 Lyses of cells

The cells were lysed by using a High pressure homogenizer (HPH) machine (Avestin C3). Cells were suspended in cell lyses buffer (50 mM Tris-HCl pH 7.6, 50 mM NaCl, 1 mM $MgCl_2.6H_2O$, 1 mM Phenyl methyl sulfonyl fluoride (PMSF), 5 mM Beta-mercaptoethanol (BME), 10% (w/v) Glycerol, 1 μM Adenosine Triphosphate (ATP)) in a cold room.

Another type of salt was also used in lyses buffer to check the better purification result of the desired protein MgtB. 200 mM of KCl and 200 mM of NaCl were also used to prepare the lyses buffer.

The cells were lysed using the Avestin emulsiflex C3 high pressure homogenizer (HPH) machine where the pressure was 15,000 psi (100 MPa) in one passage to efficiently lysed the cells. To reduce the viscosity of preparation, DNAase (1 mg/ml) was used during the cell lysed. 0.3 mM Phenyl methyl sulfonyl fluoride (PMSF) was additionally added at time of cell lysis as a Serine-protease inhibitor. After cell lysis, the cellular debris was removed by centrifugation. Centrifugation was done by using the rotor type JA 25.50 (Beckman Coulter) at 20,000 rpm for 35 minutes at 4 °C. After centrifugation cell debris was discarded and the supernatant was ultra-centrifuged.

3.1.4 Isolation of membranes

To isolate the membrane from the supernatant of the centrifuged lysate, it was ultra-centrifuged by using the rotor type 45Ti (Beckman Coulter) at 45,000 rpm for 90 minutes at 4 °C. After centrifugation, the pellet was resuspended in the membrane resuspension buffer (50 mM Tris-HCl pH 7.6, 50 mM NaCl, 1 mM $MgCl_2.6H_2O$, 5 mM Beta-mercaptoethanol (BME), 10% (w/v) Glycerol, 1 μM Adenosine Triphosphate (ATP)) and collected by using positive displacement pipette.

To check the better purification result from MgtB, 200 mM of KCl and 200 mM of NaCl were also used to prepare the membrane resuspension buffer.

Membrane pellet was homogenized gently with membrane resuspension buffer by using cylindrical glass-fiber homogenizer with teflon pestle and kept on ice. The total membrane protein concentration was adjusted to ~10 mg/ml and it was measured by using Thermo Scientific NanoDrop^{TM} 2000/2000c spectrophotometer. The concentration of protein was determined by measuring the protein absorbance at 280 nm.

3.2 Purification of protein

Protein purification process was conducted in different steps including solubilization of membrane, immobilized metal ion affinity chromatography (IMAC) for purification of Histidine-tagged recombinant protein by Ni-NTA chelating HP column (GE Healthcare) and size exclusion chromatography.

3.2.1 Membrane solubilization

The resuspended membrane solution was solubilized by adding detergent DDM (n-dodecyl beta-D-maltoside) in a ratio 1: 4 of detergent to protein (detergent: protein), where it was measured in milligrams. The solubilization was performed overnight with moderate magnetic stirring in a cold room where temperature was approximately 4 °C. While detergent can make foam in a solution, it was tried to avoid during time of mixing the detergent with membrane solution by stirring gently. 25 mM Imidazole was added additionally with membrane containing supernatant before loading onto a Ni-NTA chelating HP column to prevent unspecific binding of native proteins with the column.
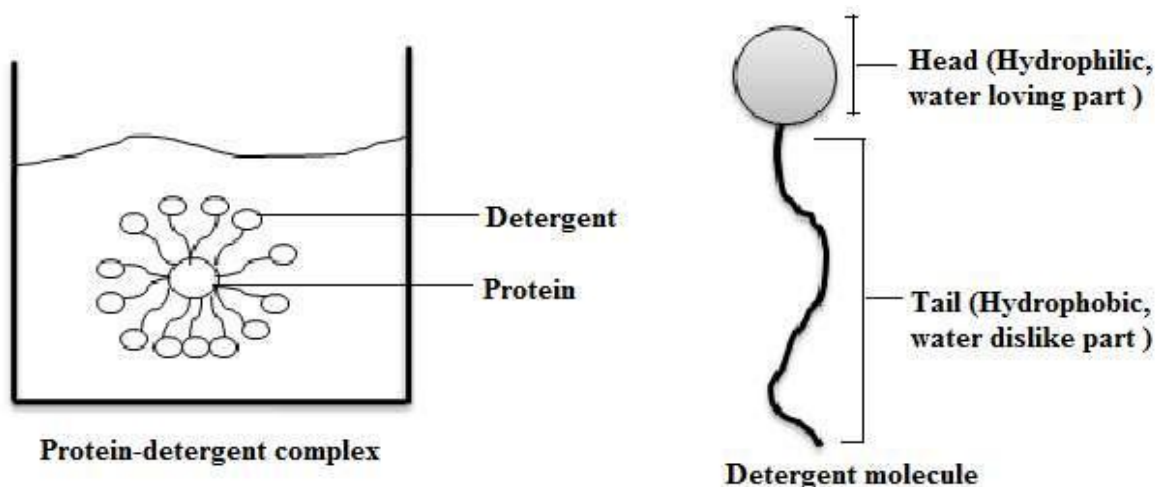

Protein-detergent complex

Detergent molecule

Figure 3.1: Solubilization of protein by detergent in solution. In picture, Right side: a drawing of how a membrane protein solubilized with detergent. Left side: a cartoon drawing of a detergent molecule that includes both a hydrophilic head group and a hydrophobic tail.

3.2.2 Immobilized metal ion affinity chromatography (IMAC)

Immobilized metal ion affinity chromatography (IMAC) is based on a high affinity binding of metal ions. Ni-NTA chelating HP 5 ml column (GE Healthcare) was used to detain the specific His-tagged protein. The column was charged with 0.1 M $NiSO_4$. Ni-NTA column was set up in a peristaltic pump (Minipuls 3, Gilson) and pre-equilibrated by 10 column volumes (cv) of the buffer A (50 mM Tris-HCl pH 7.6, 50 mM NaCl, 1 mM $MgCl_2.6H_2O$, 5 mM Beta-mercaptoethanol (BME), 10% (w/v) Glycerol, 20 mM Imidazole, 1 mM n-dodecyl beta-D-maltoside (DDM), 1 µM Adenosine Triphosphate (ATP)) before loading the sample. Then the membrane containing supernatant was loaded onto the Ni-column and after passing the supernatant through the column, 10 column volumes of washing buffer (buffer A) was used to extensively wash the column. The protein was eluted by using Imidazole to increase the concentration with a linear gradient from 100 mM to 500 mM of buffer B (buffer A+ 500 mM Imidazole). Different eluted fractions were collected by using elution buffer. These contained different concentration of Imidazole including 100 mM, 300 mM and 500 mM and every fraction was contained 5 ml elution buffer with MgtB protein. 10 eluted fractions were collected in total and the presence of MgtB protein in samples was checked by SDS-Polyacrylamide Gel Electrophoresis (PAGE) method by looking after the molecular mass of the protein.

200 mM KCl and 200 mM NaCl were also used in preparation of buffer A and buffer B to check better purification of MgtB from Ni-column.
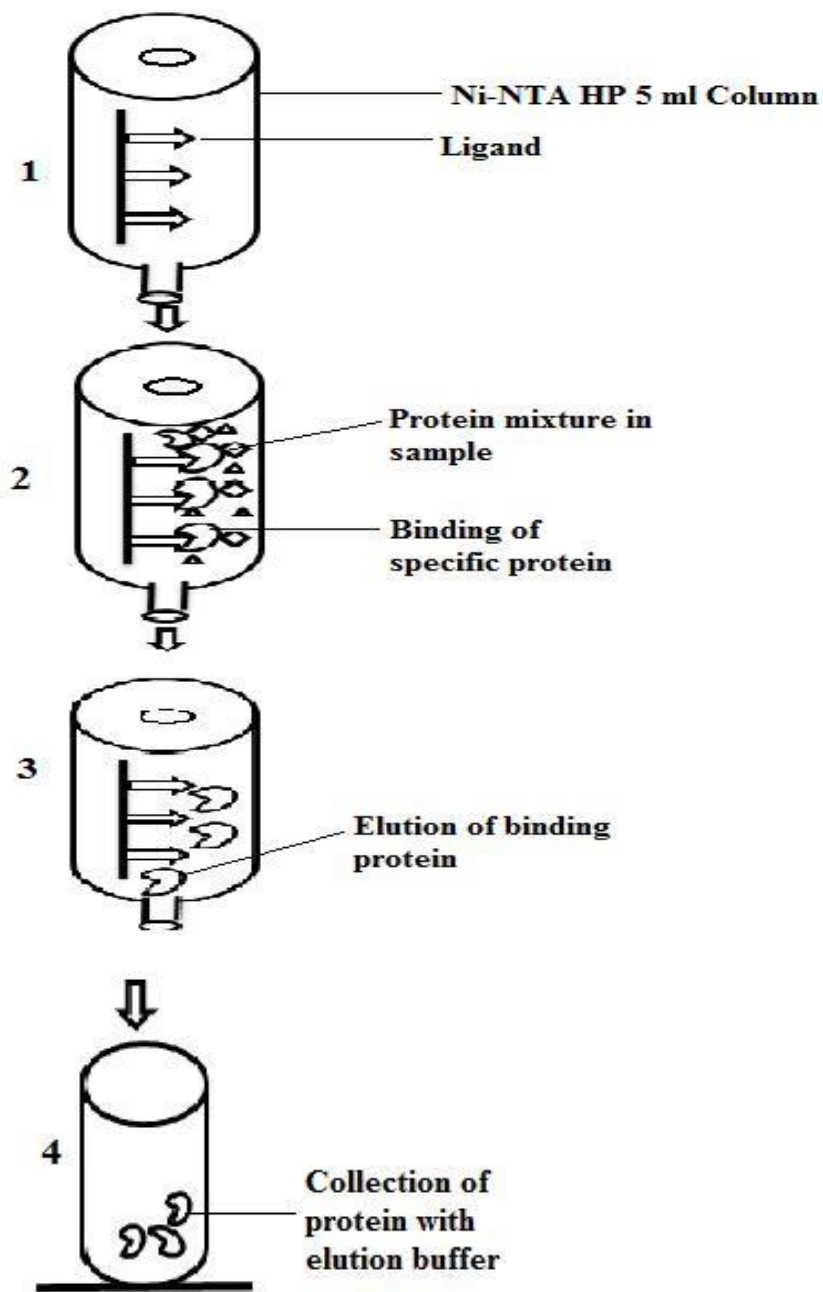
Figure 3.2: Immobilized metal ion affinity chromatography (IMAC). In step 1, equilibration of affinity column by binding buffer; step 2, sample is running through column and binding of specific His-tagged protein with binding substance or ligand; step 3, elution of binding protein though column; step 4, collection of protein with elution buffer.

3.2.3 SDS-Polyacrylamide Gel Electrophoresis (PAGE)

Electrophoresis is a method where the dispersed particles moved under the influence of electric field in solution. SDS-Polyacrylamide Gel Electrophoresis (SDS-PAGE) is one of the more popular separation methods used to separate proteins according to their molecular weight in SDS-PAGE gel. In a native state, protein contains a compact fold. To get an accurate measurement of the desired protein's molecular weight in gel, it is necessary to denature the protein. As an amphipathic surfactant, sodium dodecyl sulfate (SDS) is the most commonly used detergent to denature the proteins and contains full of negative charge. In the preparation of the loading buffer and SDS-PAGE gel, 10% (w/w) SDS was used. After adding the SDS with protein sample, the protein was solubilized and bound with the detergent uniformly. By the charge of SDS, it created a charge to molecular mass ratio between proteins in consistently. As a result, separation of proteins by the presence of SDS in polyacrylamide gel occurred by the molecular mass of the protein. In the present study, 10 eluted fractions from Ni-NTA column was prepared with 5x Loading buffer (0.2 M Tris-HCl pH 6.8 at 25 °C, 20% (w/v) Glycerol, 10% (w/w) sodium dodecyl sulfate (SDS), 10 mM Dithiothreitol (DTT), 0.05% (w/v) Bromophenol blue). In the electrophoresis method 12% SDS-PAGE gel was used to separate and detect protein as well as purified protein. After preparing, the sample was loaded onto the gel wells and was run normally at 45 mA constant current for 40 minutes until the loading sample in wells were fully disappeared. Separated protein bands were visualized by staining with Coomassie blue reagent and later destined by 10% (w/v) Acetic acid. The size of protein in gel was estimated and the gel picture was taken by using molecular imager ChemiDoc XRS $^{+}$ Imaging system (Bio-Rad).

3.2.4 Determination of MgtB Protein molecular weight through SDS-PAGE

To determine the molecular weight of MgtB protein through SDS-PAGE method, a standard curve was used. A standard curve was prepared by plotting the Log of known molecular weight of protein marker against the mobility of the protein in SDS-gel. The mobility of protein in SDS-gel was defined by the migration distance of band divided by (÷) migration distance of the dye front. After plotting the log of known molecular weight against the mobility of protein in the standard curve, a linear relationship was observed.

The equation of relative protein mobility in SDS-gel is given below.

Mobility of protein= Migration distance of band (cm) ÷ Migration distance of dye front (cm)
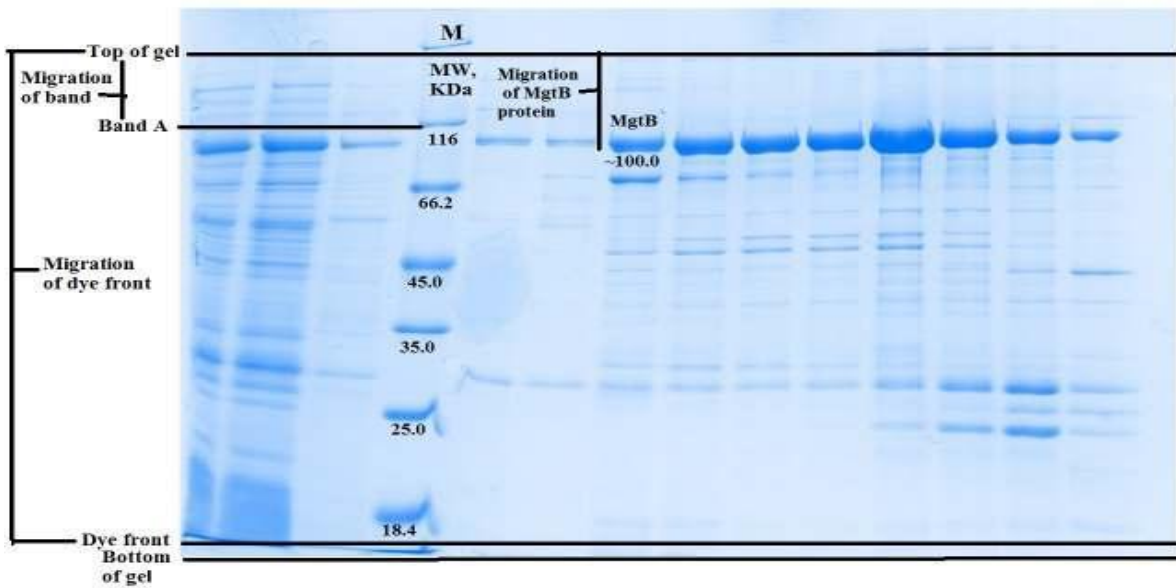
Figure 3.3: Separation of protein band with known molecular weight (KDa) in protein marker through SDS-PAGE in gel. This picture helps to calculate the relative protein mobility in SDS-gel. In picture, lane M=marker labeled with known molecular weight (KDa), lane MgtB= MgtB protein band labeled with molecular weight ~100.0 KDa.
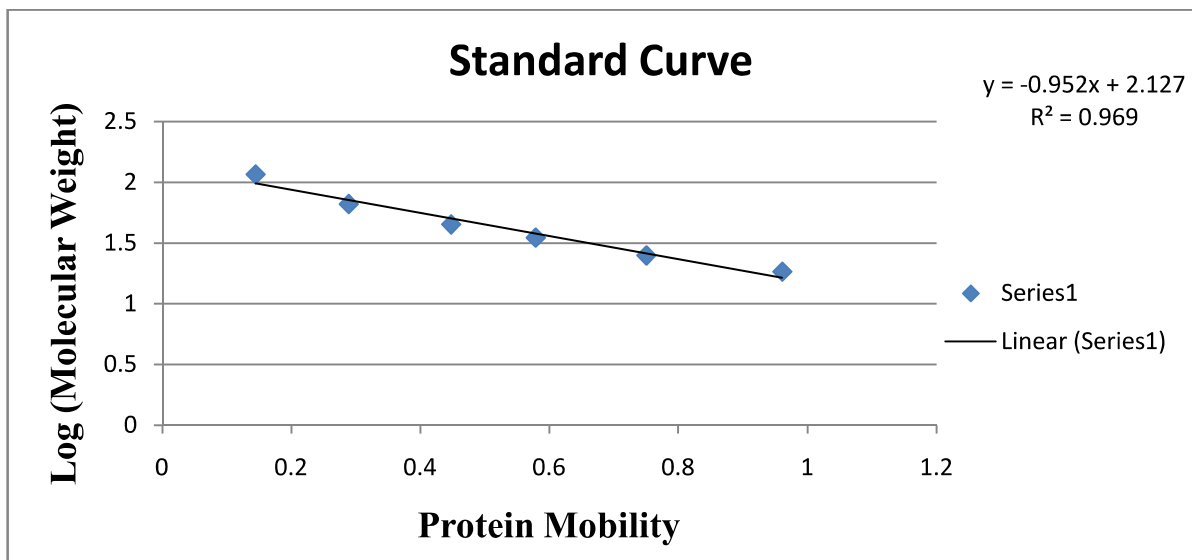
Figure 3.4: Relationship between Log of protein molecular weight and mobility of protein in SDS-gel through SDS-PAGE. The linear curve shows a linear equation y=-0.952x + 2.127 and value for regression linear in standard curve is R^2= 0.969.

By using the standard curve, molecular weight of MgtB protein was calculated.

3.2.5 Addition of tobacco-etch virus (TEV) protease and dialysis of protein sample

After checking the concentration of the protein band in gel, the elution fraction of Imidazole gradient was poured together which formed the best protein concentration. To remove the 6x polyhistidine tags (His-tag) from the N-terminal, the collected fractions of Imidazole gradient were treated with tobacco-etch virus (TEV) protease. Optimized amounts of TEV protease were added with the protein sample, in a ratio of TEV protease to total protein concentration in sample (protease: protein concentration) of 1:100. The protein sample was dialyzed to reduce the Imidazole concentration in the sample. After adding the protease and protein sample together, the sample was poured in a dialysis tube (0.3 cm/ml) with both sides tightly closed with using dialysis clip. The sample was dialyzed in dialysis buffer (50 mM Tris-HCl pH 7.6, 50 mM NaCl, 1 mM $MgCl_2.6H_2O$, 5 mM Beta-mercaptoethanol (BME), 10% (w/v) Glycerol, 1 μM Adenosine Triphosphate (ATP)) in excess with minimum of 50 times more volume of protein sample with moderate magnetic stirring in cold room where temperature was approximately at 4 °C for 16 hours or overnight.

3.2.6 Cleavage of 6x polyhistidine tag (His-tag)

The cleaved N-terminus and TEV of MgtB was separated from protein by reapplying the protein solution onto the Ni-NTA column (5 ml, GE Healthcare) and flow-through was collected. In our present study, 5 ml of His A buffer was additionally run with the flow-through of protein solution to collect whole protein solution from the tube of Ni column running peristaltic pump (Minipuls 3, Gilson). Before applying the reaction mixture onto Ni-NTA column, 30 mM Imidazole was added with the protein solution to prevent unspecific binding of proteins within the column. To check the cleaved N-terminus and TEV from protein that was captured in the Ni-NTA column, was eluted by elution buffer (buffer A+ 500 mM Imidazole). The cleaved protein in flow-through and the eluted buffer containing TEV with His-tag were analyzed by SDS-PAGE method.
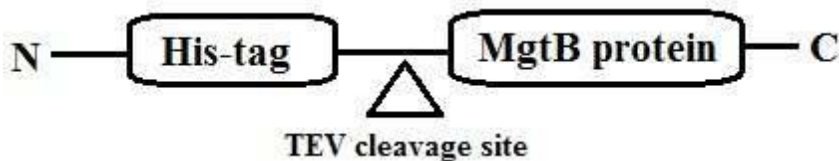

Figure 3.5: N-terminally His-tagged MgtB protein. TEV proteases cleaved in TEV cleavage site and remove the His-tag from MgtB protein.

3.2.7 Size exclusion chromatography

Size exclusion chromatography (SEC) or Gel filtration (GF) technique was used to separate MgtB protein according to the molecular size when it passes through the gel filtration column. In our present study, both the AKTA purifier and Agilent affinity system with different columns were used to check the better size exclusion chromatogram in the final purification step of the protein. Before going to run the protein sample in gel filtration (GF) technique, the protein sample was concentrated ~5.0 mg/ml by using Vivaspin 20 column (~50 kDa, cutoff, GE Healthcare) in rotor type SX4250 (BACKMAN COULTER), centrifugation at 4,000 rpm in 4 °C. To avoid the aggregation of the protein, ultra-centrifuged was done at 100,000 rpm at 4 °C for 20 minutes by using rotor type MLA-130 (BACKMAN). The concentrated protein solution was then injected into the gel filtration system.

3.2.7.1 AKTA purification

In the AKTA purifier, two types of columns were used with different salts, concentrations and detergents in gel filtration buffer. Though there was Ethanol (EtOH) in the column for decontamination, degassed distilled water (ddH$_2$O) was used to pre-wash the column. Then filtered gel filtration buffer was used to equilibrate the column. In the present study, both Superdex 200 10/300 GL and HiLoad 16/600 Superdex 200 PG (GE Healthcare) columns were used. Before loading the sample, HiLoad 16/600 Superdex 200 PG column which has a bed volume of 120 ml and average particle size is 34 μm, was equilibrated by the gel filtration buffer (10 mM Tris-HCl pH 7.6, 100 mM NaCl, 10% (w/v) Glycerol, 1 mM Dithiothreitol (DTT), 0.45 mM or 5 critical micellar concentration (CMC) of Octaethylene glycol monododecyl ether (C$_{12}$E$_8$) and 1 μM Adenosine Triphosphate (ATP)) at a flow rate 0.5 ml/min with 0.3 (MPa) pressure. 500 μl clarified concentrated protein sample was injected in the AKTA purifier system tube. Eluted fractions were collected from the fraction collector.

Another type of column Superdex 200 (10/300 GL) was also used to check the purity of the protein which had a bed volume of 24 ml and average particle size is 13 μm. In this column, 100 mM KCl, 20 mM Tris-HCl pH 7.6, 2.5 mM DTT and 1 mM DDM were used to prepare the gel filtration buffer for the equilibration of the column. 50 μl of concentrated protein sample was loaded into the system and the flow rate was 0.5 ml/min and the pressure was 1.3 (MPa).

Eluted fractions were collected from the fraction collector. Using 12% SDS-PAGE gel in SDS-PAGE electrophoresis assessed the homogeneity and purity of the MgtB protein.

3.2.7.2 Agilent purification

Agilent affinity system was also used for analytical size exclusion chromatography of the protein. The gel filtration buffer (100 mM NaCl, 10 mM Tris-HCl pH 7.6, 1 mM DTT and 0.45 mM $C_{12}E_8$, 10% (w/v) Glycerol and 1 μM Adenosine Triphosphate (ATP)) was used to equilibrate the TSKgel G3000SW (Tosoh) column which was connected to the Agilent HPLC 1260 infinity system, with a column bed volume of 26.51 ml. The column also consists of 13 μm average particle size, molecular range 1×10^4 to 5×10^5 Da and pore size 250 Å. 100 μl of protein sample was injected into the system with a flow rate of 0.5 ml/min and maximum pressure of 48 bars. Eluted fractions were collected from the fraction collector. The same Tosho column but with different gel filtration buffer composition (400 mM NaCl, 20 mM Tris-HCl pH 7.6, 10% (w/v) Glycerol and 1 mM DDM) was also used to calibrate the column. Purity of the protein in eluted fractions was assessed by SDS-PAGE electrophoresis.

3.3 Assay test

3.3.1 Liposome formation

MgtB liposome formation was required prior to check the ATPase activity of MgtB. 20 mg of DOPC and 3 mg of Cholesterol were dissolved in 2 ml of Liposome formation buffer (100 mM K_2SO_4, 100 μM Ethylenediaminetetraacetic acid (EDTA) pH 8.0 and 20 mM Tris-HCl pH 8.3). The mixture was heated for 10 minutes at 37 °C water bath. The lipid suspension was sonicated at 30 second pulse on and 60 second pulse off for 60 cycles. Then the lipid suspension was passed through o.2 μM polypropylene filter 30 times. After that, 54 μl of Triton X-100 (Bio-Rad) was added to the 2 ml liposome and mixed gently at 4 °C over night. MgtB was added to the lipid-detergent mix at the following ratio (w/w) lipids:MgtB = 20:1 and was incubated at 4 °C for 30 minutes. Detergent was removed by adding 400 mg of Bio-Beads SM-2 adsorbents (washed 1 time with methanol, 3 times with EtOH and 3 times with MilliQ water) and mixed gently at 4 °C over night. Next day supernatant was collected and stored at 4 °C.

3.3.2 Activity assay of MgtB protein

To check the ATPase activity of MgtB, 45 µl of MgtB liposome was mixed with 5 µl of ATP (stock 10 mM) in 96-well plate and incubated for 2 hours at 37 °C. The reaction was stopped by adding 75 µl of stop solution (0.25g L-Ascorbic acid dissolved in 4.15 ml H_2O and added 4.15 ml of 1M HCl, 10% Ammonium hepta-Molybdate tetra-hydrate and 20% SDS; solution was kept in ice). The plate was incubated at room temperature for 15 minutes. Then 125 µl of Bismuth citrate solution (3.5% Bismuth citrate, 3.5% Tri-sodium citrate, 1M HCl) was added and again incubated for 5 minutes at room temperature. To read the 96-well plate, eye visualization technique was used.

3.3.3 MgtB protein concentration determination by Bradford assay

MgtB protein concentration was determined by using Bradford assay, where a standard curve was made to plot some of the known protein concentrations on the curve. Known protein concentrations were detected by the absorbance and compared with the absorbance of MgtB protein solution to get the MgtB protein concentration. To prepare the standard curve, the known and commonly used protein, Bovine Serum Albumin (BSA) was diluted to make different concentrations. In the present study, 0.1 ml of each dilution of BSA was prepared in different concentration (Stock 2 mg/ml) including, 0 mg/ml, 0.125 mg/ml, 0.250 mg/ml, 0.500 mg/ml, 0.750 mg/ml, 1.000 mg/ml, 1.250 mg/ml and 1.500 mg/ml and the concentration was measured by Nanodrop spectrophotometer using absorbance at 595 nm. The known protein concentrations were plotted in a graph to make a standard curve using Microsoft Excel.

The Standard curve was prepared by plotting the absorbance of protein against the different concentration of known protein Bovine Serum Albumin (BSA) and a linear relationship was observed.
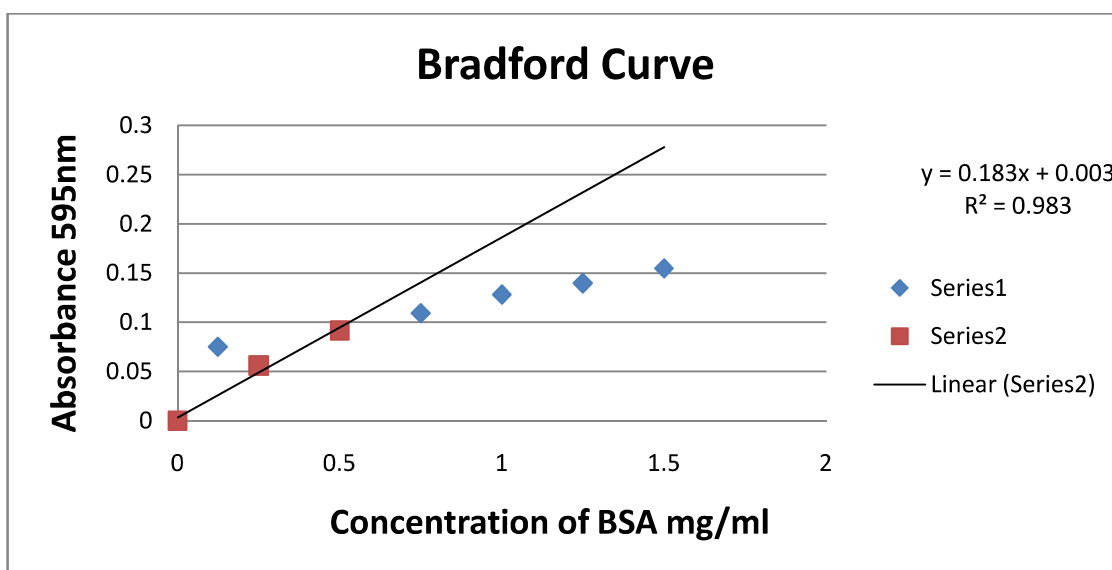
Figure 3.6: Relationship between Absorbance of protein and concentration of BSA protein. The linear curve shows a linear equation y=0.183x + 0.003 and value for regression linear in standard curve is R^2= 0.983.

After producing the linear curve, the value of the MgtB protein absorbance was plotted on the equation from linear curve to get the concentration.

3.4 Crystallization and data collection

Prior to crystallization, the protein was concentrated to ~3 mg/ml by using Vivspin 2 column (~100 kDa, cutoff, GE Healthcare) in rotor type SX4250 (BACKMAN COULTER), centrifugation at 4,000 rpm at 4 °C. Two most common techniques of hanging drop and sitting drop were used to grow the MgtB protein crystal.

3.4.1 Hanging-drop and sitting-drop techniques

MgtB protein was attempted to crystallize by using hanging-drop and sitting-drop vapor diffusion methods with different commercially available screens. In the present study, the commercially screens: MemGold[TM], MD 1-39, Box 1 of 2; MemGold[TM], MD 1-39, Box 2 of 2 and MemSys[TM], MD 1-25; (Molecular Dimension Limited) were used to grow the protein MgtB crystals. Both hanging-drop and sitting-drop crystal growth plates were taken and 250 µl of different solutions from screen were placed on different wells of plate. In the hanging-drop plate, 1 µl of protein solution drop was placed on a glass cover slip and 1 µl of reservoir

solution drop was mixed together with the cover slip protein drop by avoiding air from the pipette tip. Then the glass cover slip was sealed on the specific well by using grease or silicon oil for equilibrating the protein mixture drop against the reservoir solution. In the sitting-drop plate, 1+1 µl drops of protein and reservoir solution mixture were placed on top of the pedestal of each well and equilibrated against the 250 µl of the different reservoir solutions. The plate was then sealed by a plastic tap. Both hanging-drop and sitting-drop plates were kept in 12 °C oven (Temptech).

4. Results

4.1 MgtB Protein confirmation in sample through SDS-PAGE

The presence of MgtB after Ni-Trap elution was confirmed by visualization of the separated protein bands by staining with Coomassie blue reagent and destained by 10% (w/v) Acetic acid. To measure the size of MgtB in sample, the migration length of the band was compared to a scale marked with known molecular mass called the marker. Since the isotopically average MgtB protein molecular weight is ~100.4 kDa (UniProt) and also found the molecular mass of MgtB protein in sample to be on average ~100.0 kDa in SDS-gel.

To optimize the purification result of the protein, three different buffer compositions were used before cell lyses and Ni-column run. To prepare different buffers, three different salt concentrations were used including 200 mM of KCl and 200 mM of NaCl and 50 mM of NaCl. At high salt concentration, 200 mM KCl was used as the cell lysis buffer, Ni-column pre-equilibration (His-A buffer) and elution buffer (His-B buffer) preparation. The SDS-gel picture (Figure A) is given below.

Figure A: 200 mM KCl
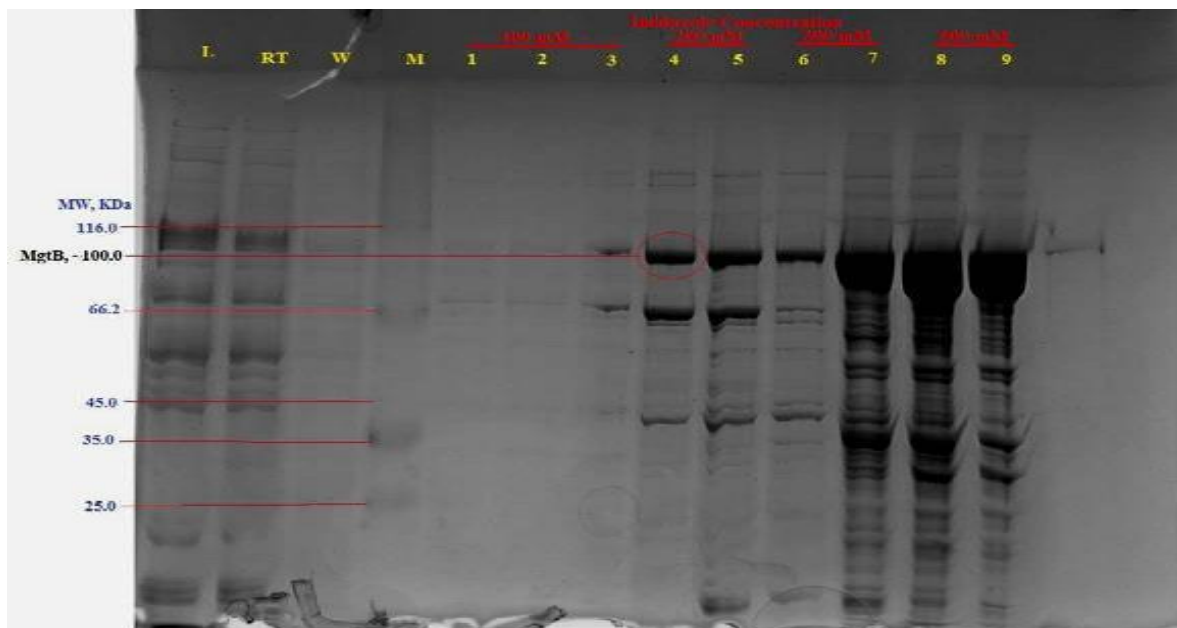
At high salt concentration, 200 mM NaCl was also used in the cell lysis buffer, Ni-column pre-equilibration (His-A buffer) and elution buffer (His-B buffer) preparation. The SDS-gel picture (Figure B) is given below.

Figure B: 200 mM NaCl
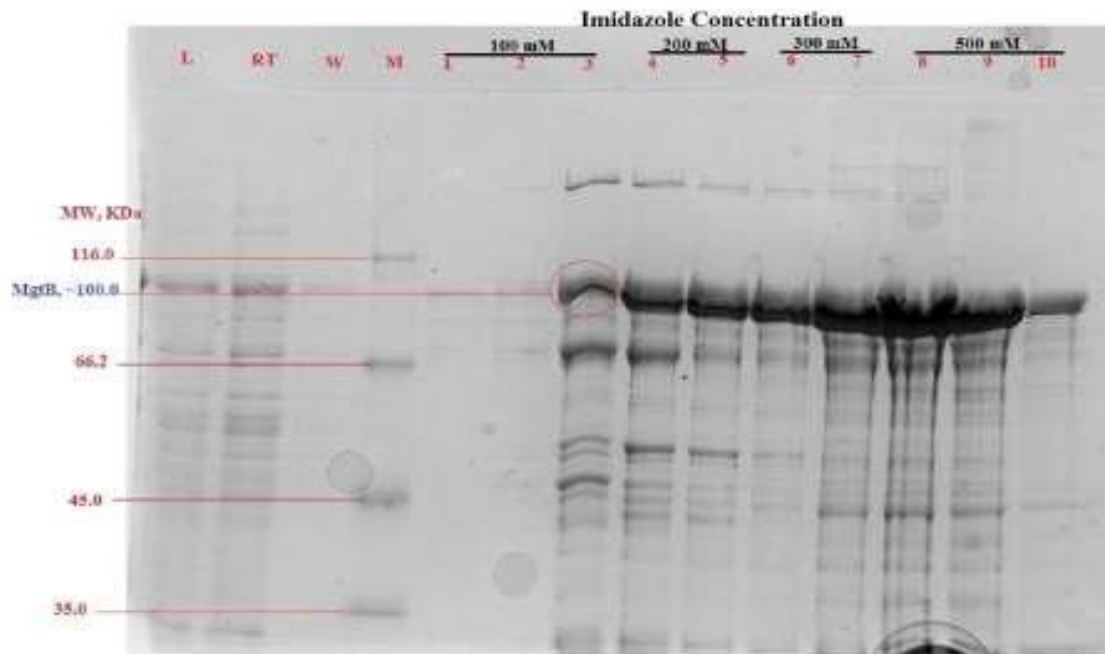
At low salt concentrations of 50 mM NaCl, additional ATP was also used in cell lysis buffer, Ni-column pre-equilibration (His-A buffer) and elution buffer (His-B buffer) preparation. The SDS-gel picture (Figure C) is given below.

Figure C: 50 mM NaCl

Figure 4.1: MgtB Protein confirmation in sample through SDS-PAGE. All figures show the coomassie blue staining SDS-gel, the presence of MgtB protein in Ni-column elusion solution by using different buffer compositions (A) 200 mM KCl; (B) 200 mM NaCl and (C) 50 mM NaCl with additional ATP. In figures differ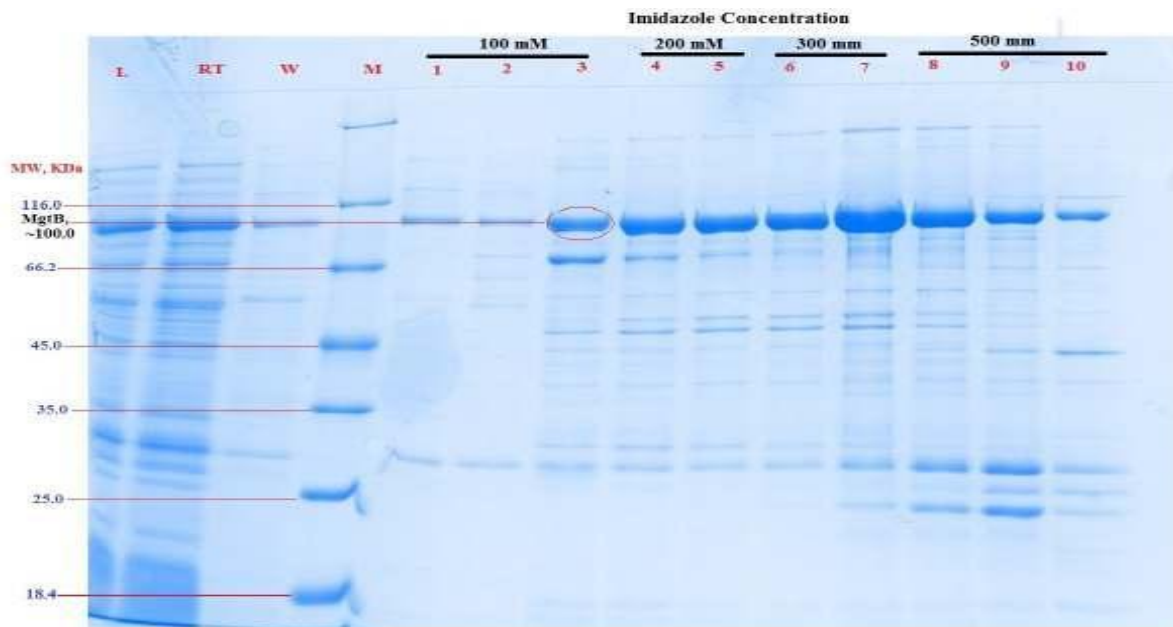ent symbols in different lanes remark as L: Load, RT: Run through, W: Wash, M: Marker labeled with known molecular weight (kDa), Lane 1-10: different fractions of elution.

Though different buffer compositions were used to lyse the cell, solubilization and purification of the MgtB membrane protein by Ni-column, in all three pictures A, B and C (Figure 4.1) have shown that the band size visualized in different lanes of eluted fractions is about ~100.0 kDa which is approximately the same as the size of MgtB. Different fractions were collected at the same amount of 5 ml elution buffer where the concentration of the Imidazole was different. The eluted fraction number 1, 2 and 3 contained 100 mM of Imidazole; fraction number 4 and 5 contained 200 mM of Imidazole; fraction number 6 and 7 contained 300 mM of Imidazole; fraction number 8, 9 and 10 contained 500 mM of Imidazole. In gel pictures A, B and C (Figure 4.1), MgtB protein band has been detected in most of the eluted fractions. But in some fractions MgtB protein has not been detected because the Imidazole concentration was not high enough in the elution buffer to elude the MgtB protein from Ni-column. Most of the MgtB proteins were eluted when the Imidazole concentration were 200 mM and 300 mM in elution buffer.

4.2 Determination of MgtB Protein molecular weight through SDS-PAGE

By using the standard curve (Figure 3.4), the molecular weight of MgtB protein has been found after calculation. From SDS-gel the MgtB protein mobility was found 0.184. By using the equation from standard curve, the molecular weight of MgtB protein was found to be ~90 kDa, even though the expected molecular weight of MgtB was ~100.0 kDa.

4.3 Confirmation of His-tag removal from MgtB protein through SDS-gel

The 6x polyhistidine tag (His-tag) was separated from the N-terminus of the MgtB protein sequence by TEV protease to cleave the TEV site and after the TEV cleavage MgtB protein was collected as a run-through by applying the mixture solution onto the Ni-column. The binding His-tag on the column was eluted by His B buffer (His A+ 500 mM Imidazole) and was

collected in total 5 fractions of 5 ml each. The run-through and the eluted fractions containing His-tag were analyzed in SDS-gel by SDS-PAGE method.
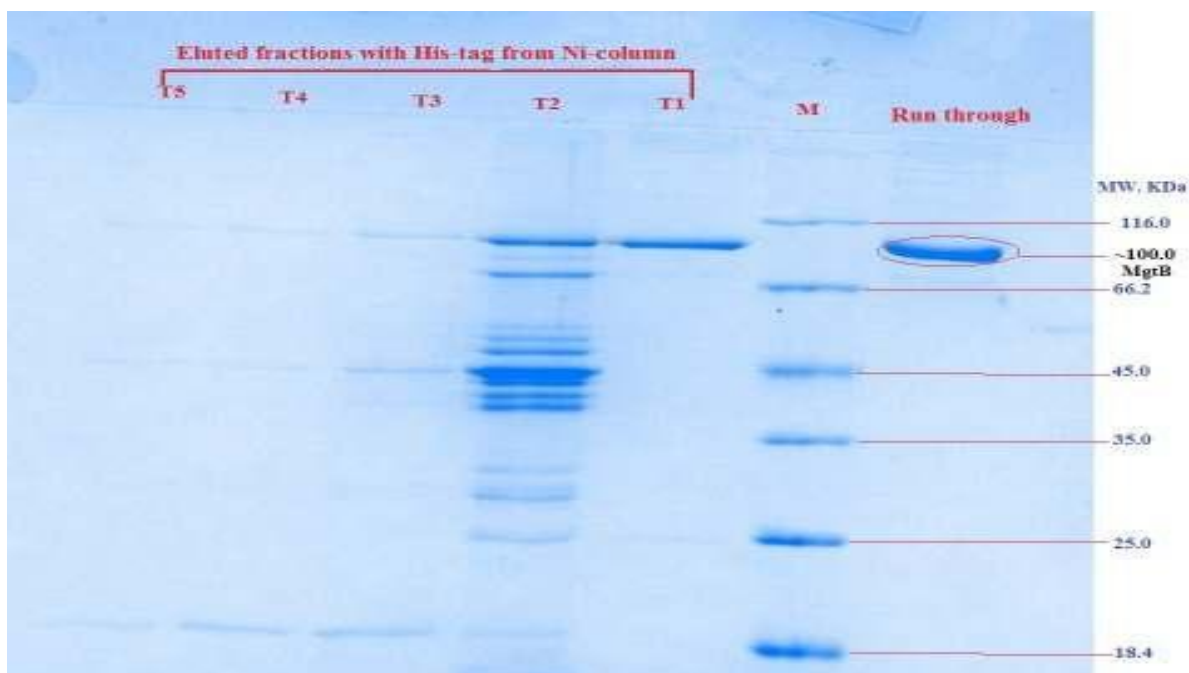
Figure 4.2: SDS-PAGE gel picture of TEV cleavage of MgtB protein. The picture shows high intensity of MgtB protein band without His-tag and 5 fractions (T1-T5) of elution of TEV with low intensity of MgtB protein and other impurities. In picture, different symbols in different lanes marked as M: Marker labeled with known molecular weight (kDa), Lane Run-through: MgtB after removal of His-tag, Lane T1-T5: Different fractions containing His-tag.

4.4 Size exclusion chromatography

4.4.1 AKTA purification

HiLoad 16/600 Superdex 200 PG (GE Healthcare) column was used in the final size exclusion chromatographic step and the separation buffer (10 mM Tris-HCl pH 7.6, 100 mM NaCl, 10% (w/v) Glycerol, 1 mM Dithiothreitol (DTT), 0.45 mM or 5 critical micellar concentration (CMC) of Octaethylene glycol monododecyl ether ($C_{12}E_8$) and 1 μM Adenosine Triphosphate (ATP)) was used in the column.

Figure 4.3: Chromatogram from column HiLoad 16/600 Superdex 200 PG (GE Healthcare). The picture shows the chromatographic separation of proteins in final purification step by using AKTA explorer system. Void volume (V_o) was found at 45 ml and the UV absorption of protein at 280 nm.

In the chromatogram, HiLoad 16/600 Superdex 200 PG showed high resolution of protein detection at time of running the buffer elution between 48 ml to 70 ml. Eluted fractions were collected from the fraction collector and analyzed by 12% SDS-PAGE gel to check the purity of MgtB protein. SDS-gel pictures are given below.

Figure A: Fraction no. C3 to C13 (HiLoad 16/600 Superdex 200 PG)

Figure B: Fraction no. C14 to D9 (HiLoad 16/600 Superdex 200 PG)
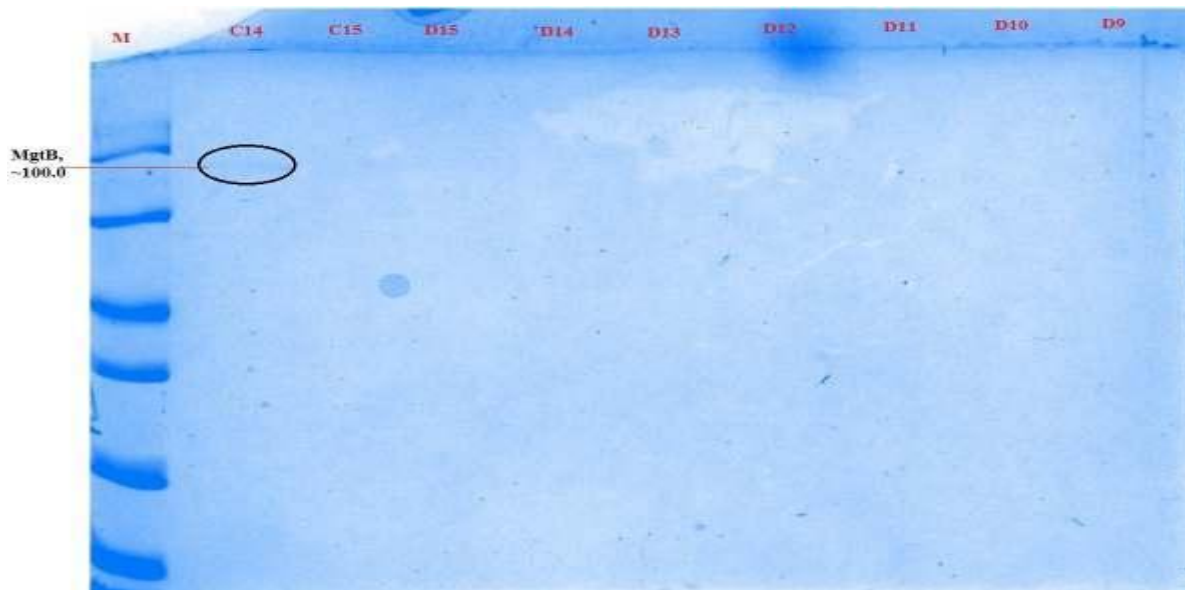
Figure 4.4: Detection of MgtB protein by analysis of column HiLoad 16/600 Superdex 200 eluted fractions. The pictures (Figure A and B) show the collected elution fractions analysis from AKTA purification by SDS-PAGE to detect MgtB protein band in Coomassie blue

staining SDS-gel from 48 ml to 70 ml eluted fractions of running buffer. Lane M shows the size marker. In picture A and B, other lanes C3 to D9 show different elution fractions.

Another column, Superdex 200 10/300 GL was also used to separate the proteins and to obtain better purified MgtB protein in the final purification step. The salt and detergent were changed in the separation buffer (100 mM KCl, 20 mM Tris-HCl pH 7.6, 2.5 mM DTT, 10% (w/v) Glycerol and 1 mM DDM) of the column.
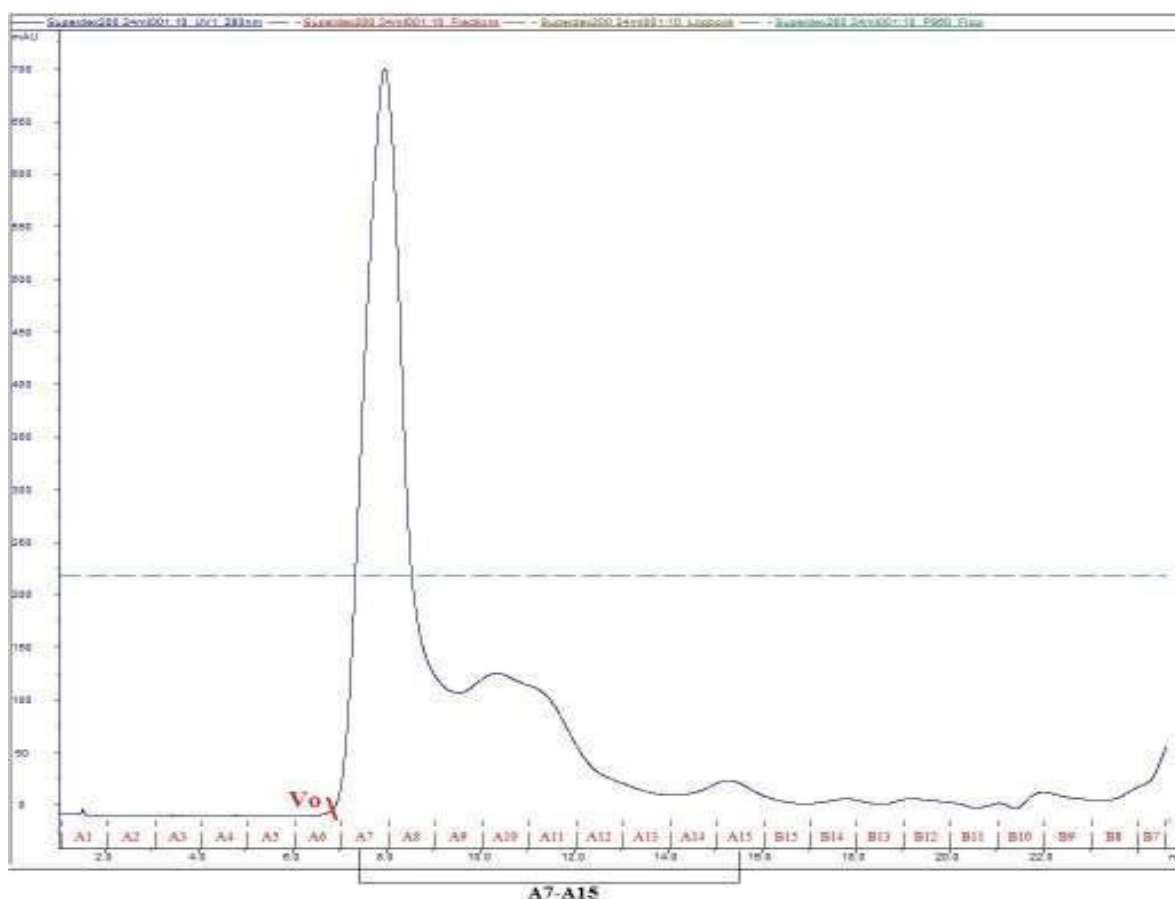
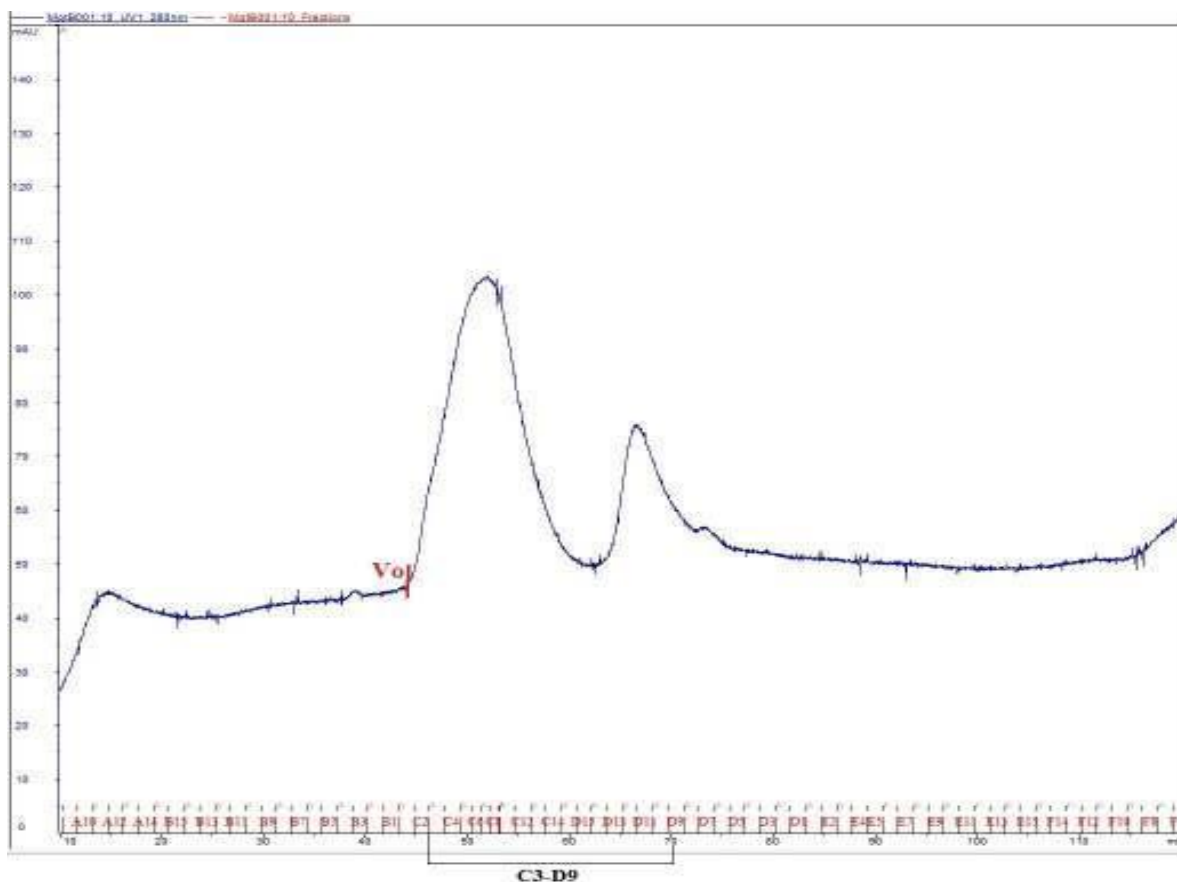**Figure 4.5: Chromatogram of Superdex 200 10/300 GL (GE Healthcare).** The picture shows the chromatographic separation of proteins in final purification step by using AKTAexplorer system. Void volume (V_o) was found at 7 ml and the UV absorption of protein at 280 nm.

In the chromatogram, Superdex 200 10/300 GL showed poor resolution of protein detection at time of running the buffer elution between 7 ml to 15 ml. Eluted fractions were collected from

the fraction collector and analyzed by 12% SDS-PAGE gel to check the purity of MgtB protein. SDS-gel picture is given below.
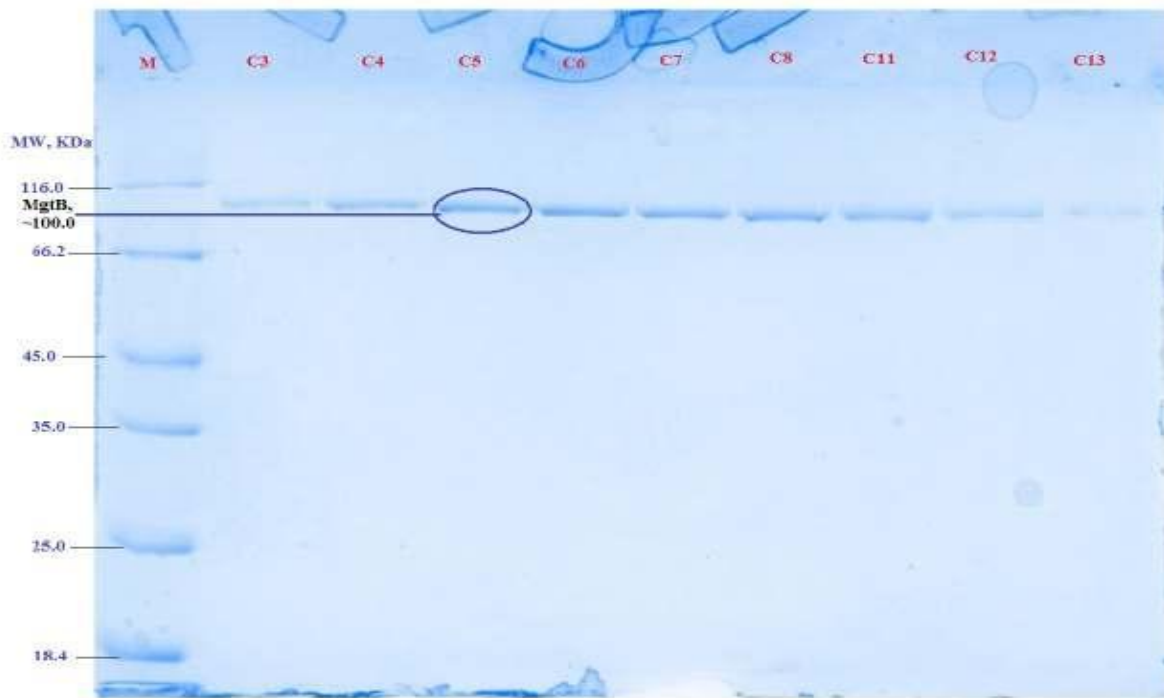
Figure: Fraction no. A7 to A15 (Superdex 200 10/300 GL)

Figure 4.6: Detection of MgtB protein by analysis of column Superdex 200 10/300 GL eluted fractions. The picture shows the collected elution fractions analysis from AKTA purification by SDS-PAGE to detect MgtB protein band in Coomassie blue staining SDS-gel from 7 ml to 15 ml eluted fractions of running buffer. Lane M shows the size marker and other lanes A7 to A15 show different elution fractions.

After analysis of collected fractions from two different columns (chromatogram showed in figure 4.3 and 4.5) in SDS-gel, MgtB protein band has been found in all collected fractions except in Figure 4.4 (B) fraction number C15 to D9, though there was a good peak in the chromatogram. By using two different salts and detergents in final purification step of MgtB, it can be concluded that the protein MgtB is more stable and soluble in salt 100 mM NaCl with detergent 0.45 mM $C_{12}E_8$ rather than 100 mM KCl with detergent 1 mM DDM.

4.4.2 Agilent purification

In analytical size exclusion chromatographic method TSKgel G3000SW (Tosoh) column connected with Agilent HPLC 1260 infinity system was used to separate and purify the MgtB protein. In column, the separation buffer composition was 100 mM NaCl, 10 mM Tris-HCl pH 7.6, 1 mM DTT and 0.45 mM $C_{12}E_8$, 10% (w/v) Glycerol and 1 µM Adenosine Triphosphate (ATP).
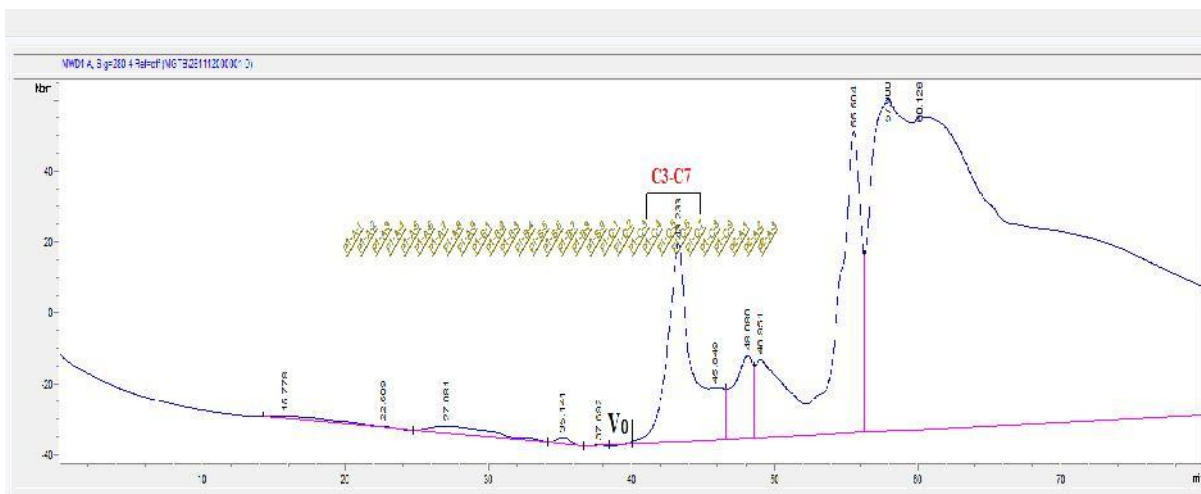
Figure 4.7: Chromatogram of TSKgel G3000SW (Tosoh). The picture shows the analytical size exclusion chromatographic separation of proteins step by using Agilent HPLC 1260 infinity system and the UV absorption at 280 nm. Void (V_o) was found after 40 min of run.

In chromatogram, TSKgel G3000SW (Tosoh) showed high resolution of protein separation in time of running the buffer elution between 40 to 45 minutes. Eluted fractions were collected from the fraction collector and analyzed by 12% SDS-PAGE gel to check the purity of MgtB protein. SDS-gel pictures are given below.
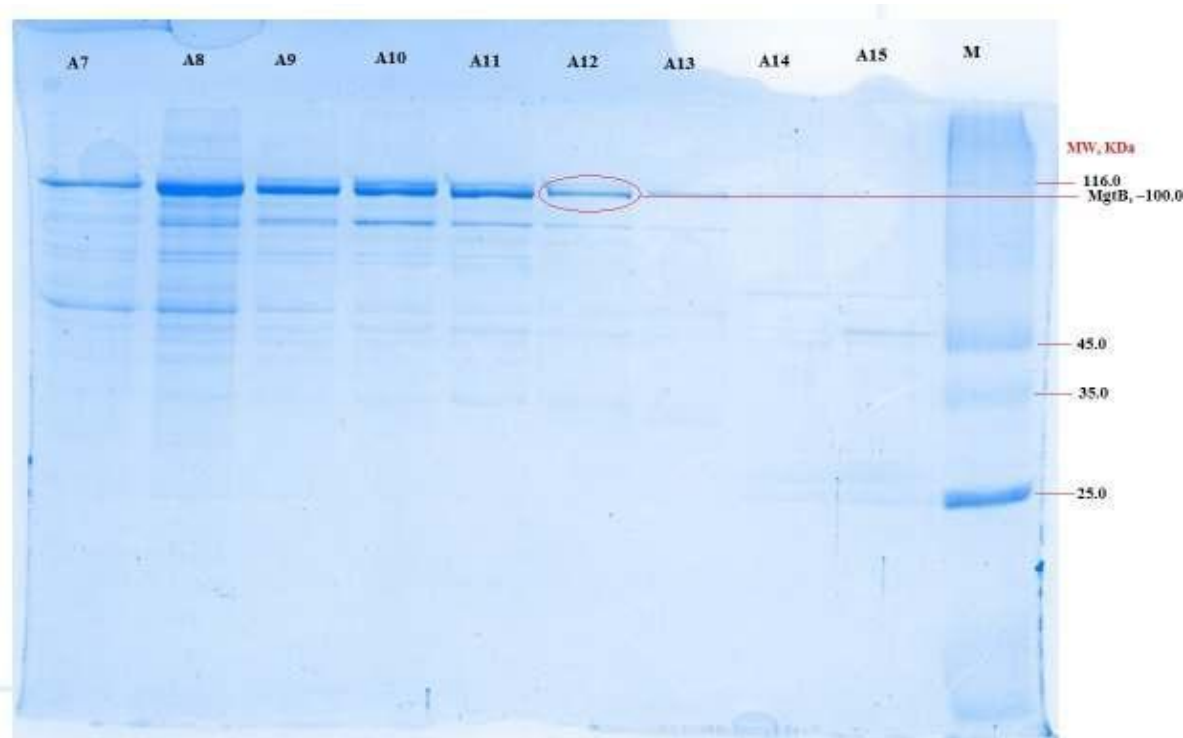
Figure 4.8: Detection of MgtB protein by analysis of column TSKgel G3000SW (Tosoh) eluted fractions. The picture shows the the collected elution fractions analysis from Agilent purification analysis by SDS-PAGE method to detect MgtB protein band in Coomassie blue staining SDS-gel from eluted fractions of running buffer. Lane M shows the size marker and other lanes C3 to C7 show different elution fractions.

The same Tosho column but different separation buffer composition with high salt concentration and different detergent (400 mM NaCl, 20 mM Tris-HCl pH 7.6, 2.5 mM DTT, 10% (w/v) Glycerol and 1 mM DDM) was used to separate MgtB protein in column.
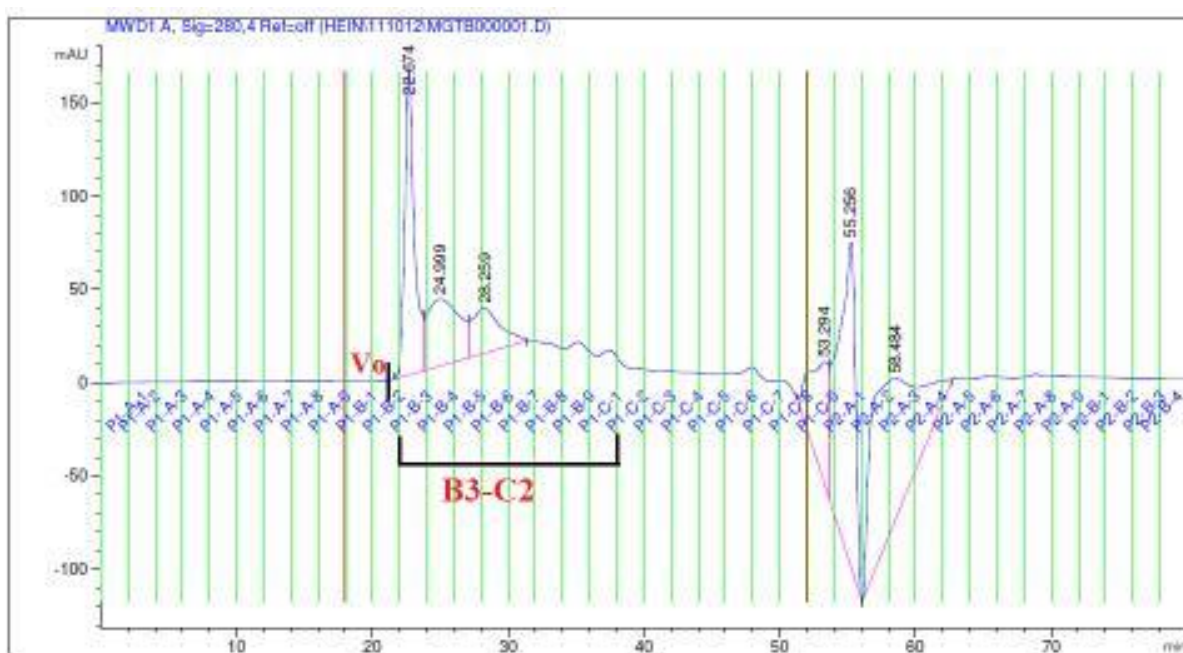
Figure 4.9: Chromatogram of TSKgel G3000SW (Tosoh). The picture shows the analytical size exclusion chromatographic separation of proteins step by using Agilent HPLC 1260 infinity system and the UV absorption at 280 nm. Void (V_o) was found after 21 min of run.

In chromatogram, TSKgel G3000SW (Tosoh) showed good resolution of protein separation in time of running buffer elution between 22 to 38 minutes. Eluted fractions were collected from the fraction collector and analyzed by 12% SDS-PAGE gel to check the purity of MgtB protein. SDS-gel pictures are given below.
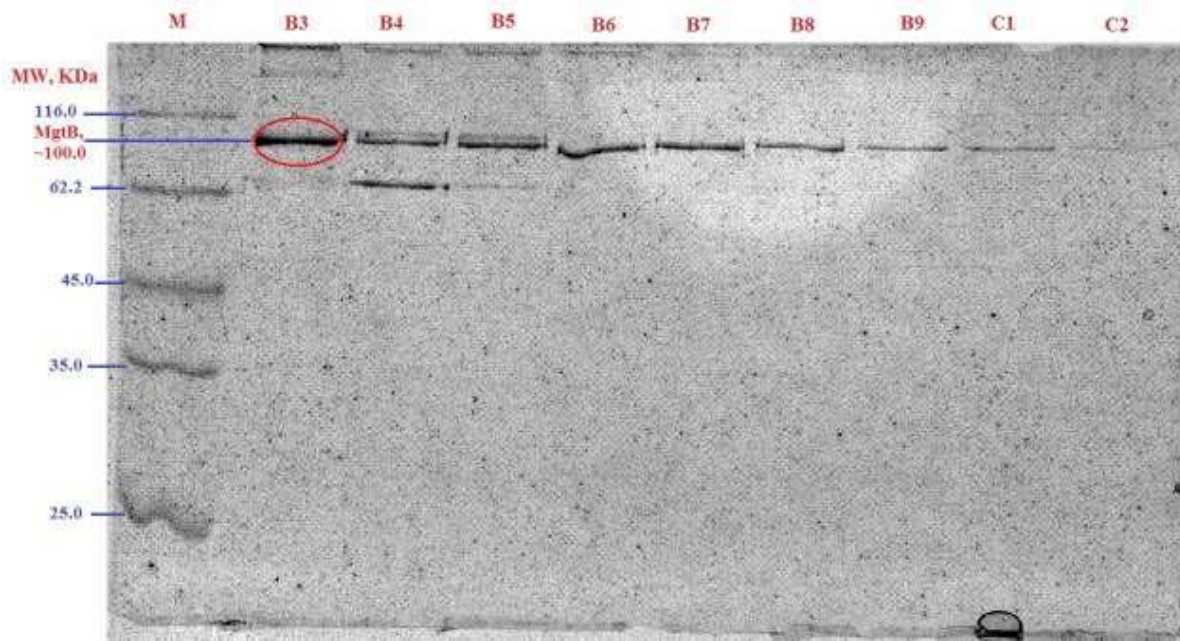
Figure 4.10: Detection of MgtB protein by analysis of column TSKgel G3000SW (Tosoh) eluted fractions. The picture shows the the collected elution fractions analysis from Agilent purification analysis by SDS-PAGE method to detect MgtB protein band in Coomassie blue staining SDS-gel from eluted fractions of running buffer. Lane M shows the size marker and other lanes B3 to C2 show different eluted fractions.

After analysis the collected fractions from same Tosoh column (chromatogram showed in figure 4.8 and 4.10) in SDS-gel, MgtB protein band has been detected in all collected fractions except in Figure 4.8, fraction number C3 to C5. By using the same salt with different detergent in different concentrations i.e. 100 mM NaCl with detergent 0.45 mM $C_{12}E_8$ and 400 mM NaCl with detergent 1 mM DDM in purification step of MgtB protein, it can be concluded that the protein MgtB is more soluble in detergent 0.45 mM $C_{12}E_8$ than detergent 1 mM DDM and nicely separated and purified by using NaCl with detergent $C_{12}E_8$ in gel separation buffer. Besides, the figure 4.10 showed some impurities including lower molecular weights protein band in SDS-gel.

4.5 Assay test

4.5.1 Activity assay of MgtB protein

The result data were collected from the 96 flat-bottom well plate of MgtB protein activity test after eye observation. After adding the Bismuth citrate solution, blue coloration was observed in some wells. Heavy precipitation was also observed in some wells which prevented the measurement at 690 nm. Having seen that some wells turned blue, it can be concluded that MgtB is active.

4.5.2 MgtB protein concentration determination by Bradford assay

After creating the linear curve (Figure 3.6), linear equation has been observed and the value of MgtB protein absorption was plotted on the equation to get the concentration of MgtB protein. The absorbance of MgtB protein was found to be 0.03 nm. By using the linear equation from the standard curve, the concentration of MgtB protein was found to be 0.15 mg/ml.

4.6 Crystallography plate observation

To find the harvestable crystals of MgtB protein, each well (hanging-drop and sitting-drop plates) was inspected under stereo light microscope (Leica M205 C; Leica Microsystem). In crystal growing plate to grow crystal of MgtB protein different types of commercial screens were used like, MemGold^{TM} MD 1-39 (Box 1 of 2), MemGold^{TM} MD 1-39 (Box 2 of 2) and MemSys^{TM} MD 1-25; (Molecular Dimension Limited). Though it was not observed any crystal of MgtB protein after observation of the crystal plate, but showed some false negative and some false positive results in the conclusion.

During the observation of crystallography plate containing MemGold^{TM} MD 1-39 (Box 1 of 2) and MemGold^{TM} MD 1-39 (Box 2 of 2) commercially screens, it showed false negative results in time of inspecting the wells of crystal plate. All of the wells showed clear drop with precipitant after mixture MgtB protein sample and buffer solution from screen. From this result, it comes to the conclusion that the different conditions of buffer from this commercial screen are not suitable for growing crystals of MgtB protein. The picture of false negative crystal is given below in figure 4.11 (C).

Some false positive results were also found from the crystallography plate during the observation. Some of the wells of the crystal plate that contained commercial screen MemSys^{TM} MD 1-25, have shown false positive results. The initial false crystal hit were

obtained in three different conditions, including MYS 2 (0.1 M NaCl, 0.1 M Lithium Sulfar, 0.1 M Sodium citrate pH 3.5, 30% v/v PEG 400), MYS 17 (0.1 M NaCl, 0.1 M Lithium Sulfar, 0.1 M Na HEPES pH 7.5, 30% v/v PEG 400) and MYS 18 (0.1 M NaCl, 0.1 M $MgCl_2$, 0.1 M Na HEPES pH 7.5, 30% v/v PEG 400). The growing crystals on those wells were checked by empty cryo-loop mounted on a pin under the microscope and the crystals were break down when it was pressed very gently by cryo-loop mounted pin. From this result, it comes to the conclusion that those crystals were produced from salts. Picture of false positive crystal is given below in figure 4.11 (D).
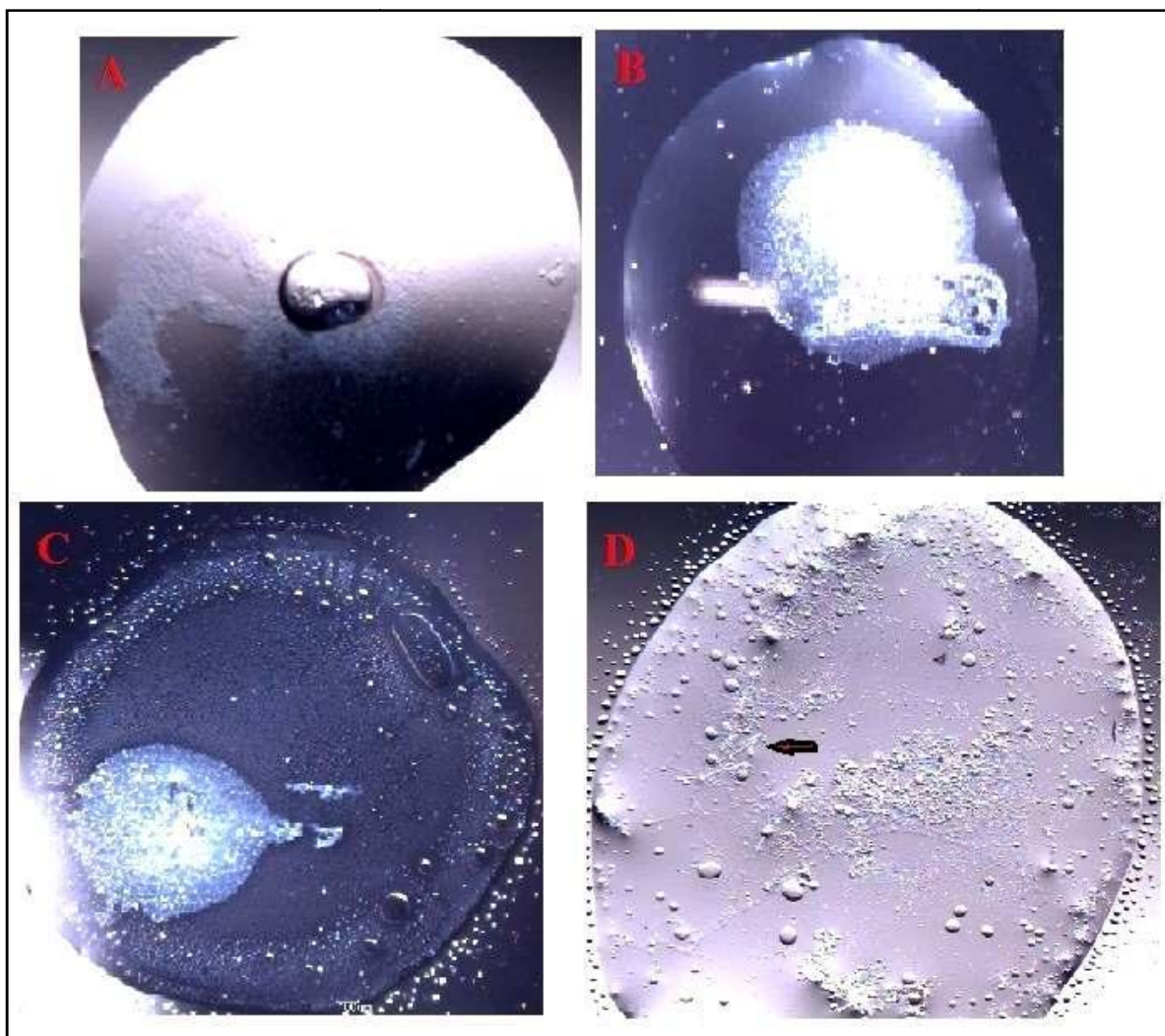
Figure 4.11: Light microscopic image of different droplet, after mixing of MgtB protein sample and different buffer condition from commercial screens: (A) drop after MgtB protein mixture with buffer, (B) clear drop after MgtB protein mixture with buffer, (C)

zoom picture of clear drop, (D) zoom picture of false positive crystal hit in droplet after MgtB protein mixture with buffer. Picture A was taken from the crystallographic plate well containing MYS 2 buffer; picture B was taken from the crystallographic plate well containing buffer MYS 38 (0.1 M NaCl, 0.1 M MOPS pH 7.0, 12% w/v PEG 400); picture C shows the zoom condition of picture B that showed the false negative result; picture D was taken from the crystallographic plate well containing MYS 17 buffer that showed salt crystal (black arrow marked) with false positive result of growing crystal.

5. Discussion

In human and most of mammals, *Salmonella typhimurium* causes gastroenteritis, also called diarrhea [39]. It is assumed that this bacterium also causes typhoid fever in human and shows some similar typhoid symptoms in mice [40]. Mg^{2+} is needed for survival of the bacterium inside macrophage. MgtB transport necessary amounts of Mg^{2+} inside bacterium with other Magnesium transporters, to overcome the lowering of Mg^{2+} concentration and helps the bacterium to survive [41]. Studying MgtB from *S. typhimurium* will help to reveal its unknown mechanism of Mg^{2+} transport along with other Mg^{2+} transporters.

5.1 Purification of MgtB Protein by Immobilized metal ion affinity chromatography (IMAC) technique

During every step of protein purification, it is necessary keep protein stable and functioning in sample solution by maintaining the buffer condition. Appropriate buffer may prevent unfolding and aggregation of protein. The factors that should be considered for optimizing buffer are pH, salt, reducing agents, stabilizing reagents etc. Proteins are generally less soluble at their isoelectric point (pI) value that represents a pH and at that point the net charge of protein is zero. Sudden changes of pH in buffer could irreversibly affect protein folding, solubility and function. The pI of MgtB was calculated from its amino acid sequence and was found to be 6.69 (ExPASy's ProtParam tool). In this experiment, pH 7.6 was used in all buffers and found that MgtB protein was stable at that pH. Tris is temperature sensitive that can change the pH of buffer at different temperature. Since Tris was used in this experiment and was mixed with other solutions at room temperature, so Tris-HCl and all other buffers were prepared and pH was measured at same room temperature.

Buffer with suitable concentration and ionic strength are also very important to make the protein soluble and active. To enhance the solubility of protein, salt was added while making different buffers. Though high salt concentration like 0.5 to 1.0 M could possibly be used while making buffers to separate proteins by Ni-affinity column but most proteins are less soluble at high salt concentration [42].

In this experimental procedure, buffers with high salt concentration at 200 mM and low salt concentration at 50 mM were used to check the better protein solubility and increase the purity of MgtB protein by IMAC technique. MgtB was collected in eluted fractions from Ni-column by changing Imidazole concentration from 100 mM to 500 mM in MgtB elution buffer. Two

types of salt, KCl and NaCl with two different concentrations 200 mM and 50 mM were used while making buffers as described in methodology part (Section 3.1.3). From Figure 4.1, A (200 mM KCl) and B (200 mM NaCl), at high salt concentration, fraction number 1 and 2 have not shown MgtB band, whereas in figure C (50 mM NaCl), at low salt concentration have shown less concentrated MgtB band. In picture A, fraction number 3 have shown less concentrated MgtB band, whereas in figure B and C have shown relatively high concentrated MgtB band in same fraction number. In all three pictures fraction number 4 to 9, at high and low salt concentration of KCl and NaCl have shown relatively equal concentrated MgtB band. In picture B and C, fraction number 10 has shown less concentrated MgtB band but in picture A, fraction number 10 was not collected. Lately it was changed in procedure and tried to elute all MgtB from Ni-column in eluted fraction. In figure 4.1, A and B, at high salt 200 mM concentration, most of the protein MgtB was eluted at Imidazole concentration 300 mM and 500 mM. On the other hand, at low salt 50 mM concentration of NaCl, most MgtB started to elute at relatively less Imizadole concentration (Figure 4.1, C) from 100 mM to 500 mM in eluted fractions.
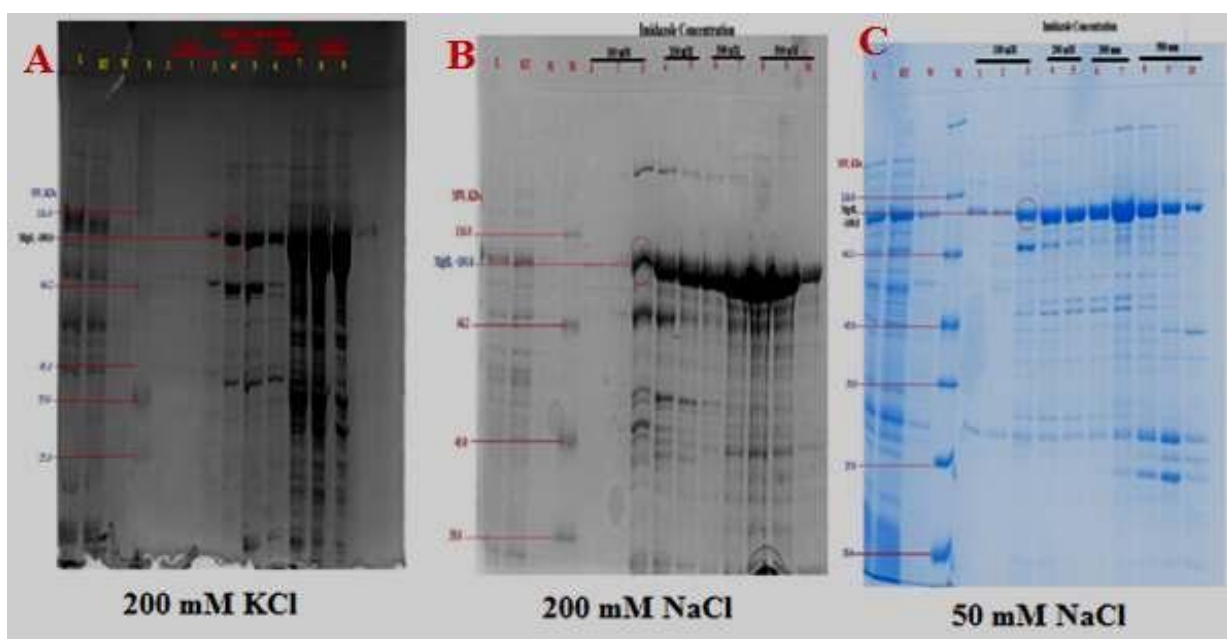

Figure 4.1: MgtB Protein confirmation in sample through SDS-PAGE.

5.2 Determination of MgtB protein molecular weight through SDS-PAGE

After analyzing all collected fractions in Coomassie blue stained SDS-gel, MgtB protein bands were detected at molecular weight approximately 100.0 kDa (Figure 3.3) using protein ladder with known molecular weight (kDa). The electrophoretic mobility of different polypeptide chains in marker were calculated by using mobility of protein formula that described in section 3.2.4 and plotted the measurement against the log of their molecular weights (Figure 3.4). By using the relative protein mobility formula, the protein mobility of MgtB was found 0.19 and the calculated molecular weight was found 90.0 kDa, even though the expected molecular weight of MgtB protein was ~100.0 kDa (UniProtKB). This difference could be because of various reasons like MgtB might not behave well like standard protein in SDS-PAGE as expected and it might not have fully unfolded after adding SDS, so the mobility of protein in gel was not well enough and the migration of protein band was not accurate in distance. MgtB might also be cleaved during protein preparation for gel electrophoresis in normal temperature as MgtB protein is temperature sensitive [12]. In the graph (Figure 3.4), some of data showed imprecise data points and was not fit on the trend line of the curve and pushed the curve nonlinear. Without minimizing this problem, this calibration graph might give a large error that will reduce the accuracy of the standard curve. To avoid such kind of problem in the present experiment, only accurate data points were considered to make the linear curve.

5.3 Confirmation of His-tag removal from MgtB protein through SDS-gel

The gene *mgtB* was cloned into vector pETM-11 with 6x polyhostidine tag and TEV protease cleavage site as N-terminal fusion. Polyhistidine-tag (6x histidine-tag) was used for affinity purification of His-tagged recombinant MgtB protein by Ni-NTA column. Since His-tag interfere with folding and structure of target protein and has influential effect on protein crystal formation [43], it should be removed from the target protein after the expression and purification steps. In this experiment, TEV proteases were used to cleave the His-tag from MgtB. TEV protease is very specific, can recognize a linear epitope of the general form Glu-Xaa-Xaa-Tyr-Xaa-Gln-(Gly/Ser), which leaves Glycine (Gly) and/or Serine (Ser) after the cleavage site [44]. At high concentration of Imidazole, the activity of TEV proteases is slow and maximally active at room temperature 34 °C but in this experiment MgtB protein was treated with TEV protease at 4 °C. Since TEV protease is three-fold less active at 4 °C [45], the duration of cleavage reaction was increased overnight while dialyzing to remove Imidazole

(section 3.2.5). To prevent the nonspecific binding of some endogenous protein to Ni-NTA column, low concentration of Imidazole (20 mM) was added to the sample and washing buffer [46]. During passing through Ni-NTA column, the MgtB containing His-tag binds to Ni-column and run through contained cleaved MgtB protein and other eluted fractions (T1-T5) contained the TEV site with His-tag (Figure 4.2). Though separation of protein bands were not fully good in figure 4.2, but the lane Run through showed high intensity of MgtB protein band with no impurities. On the other hand, the eluted fractions (T1-T5) showed less concentrated MgtB protein with His-tag and other impurities in SDS-gel picture because sometimes Ni-NTA column retains several well known proteins as impurities [47]. In SDS-gel picture (Figure 4.2), lane T1 and Run through showed quite equal protein band because Ni-NTA column was attached with a long tubing system set up with Peristaltic pump (Minipuls 3, Gilson). Because of this tubing system, little amount of samples from previous fraction possibly mixed with next fraction.

5.4 Size exclusion chromatography

There are different chromatographic protein purification methods, among them size exclusion chromatography (SEC) method is best for separating proteins according to the protein molecular size. SEC technique can easily distinguish different forms of protein like monomer, oligomeric and/or polymeric aggregation. The protein molecules are separated when it pass through the gel filtration column, the larger size of protein molecules will pass faster through the cross-linked polymer as they will not fit into the pores of polymers whereas smaller size of protein will penetrate to the pores and will take more time to pass the gel filtration column. In this present study, for size exclusion chromatography technique both AKTA purifier and Agilent affinity system were used with different gel filtration columns (section 3.2.7) to check the better size exclusion profile of MgtB. Both HiLoad 16/600 Superdex 200 PG and Tosoh column TSKgel G3000SW can separate protein according to their molecular size but have some distinct difference between them. The amount of sample loading in system depends on size of the column but comparatively it is possible to load little bit large amount of sample in HiLoad 16/600 Superdex 200 PG, AKTA purification column compare to Tosoh column TSKgel G3000, Agilent affinity column. To achieve high resolution in chromatogram, the sample volume should be less than 5% of the total volume of the column. In this present study different types of salt and detergents were used in buffer to purify MgtB from the crude sample of MgtB

protein solution. The eluted fractions were analyzed by using 12% SDS-PAGE gel to assess the purity of protein. Though the chromatogram from HiLoad 16/600 Superdex 200 PG where 100 mM NaCl salt with detergent 0.45 mM $C_{12}E_8$ were used in separation buffer (figure 4.3) showed good resolution peak, but no MgtB protein band was visualized in SDS-gel in some fractions (figure 4.4, B). This can happen that wrong fractions might be collected from the fraction collector. Apart from this on instance, fractions collected during following experiments showed relatively good concentration of MgtB protein band in SDS-PAGE gel (figure 4.4, A). 100 mM KCl salt with detergent 1 mM DDM were used in buffer for column Superdex 200 10/300 GL and the result have shown in figure 4.6. Since two different columns were used in AKTA purification system with two different salts and detergents in buffer, the comparative analysis of two chromatograms (figure 4.3 and 4.5) is not possible because the bed volume of column is not same. SDS-PAGE gel pictures (figure 4.4 and 4.6) analysis was considered to optimize the difference of using different salts with different detergents in this experiment at final purification step of MgtB protein. The SDS-gel picture, figure 4.4 did not shown any impurities or degradation of MgtB protein band in eluted fractions, whereas figure 4.6 showed many lower molecular weight band, which could be degraded product of MgtB or impurity which was not removed during the purification process. By using mass spectrometry it is possible to identify the protein degradation which was not performed here.

Fig 4.4: HiLoad 16/600 Superdex 200(NaCl and $C_{12}E_8$)   Fig 4.6: Superdex 200 10/300 GL(KCl and DDM)
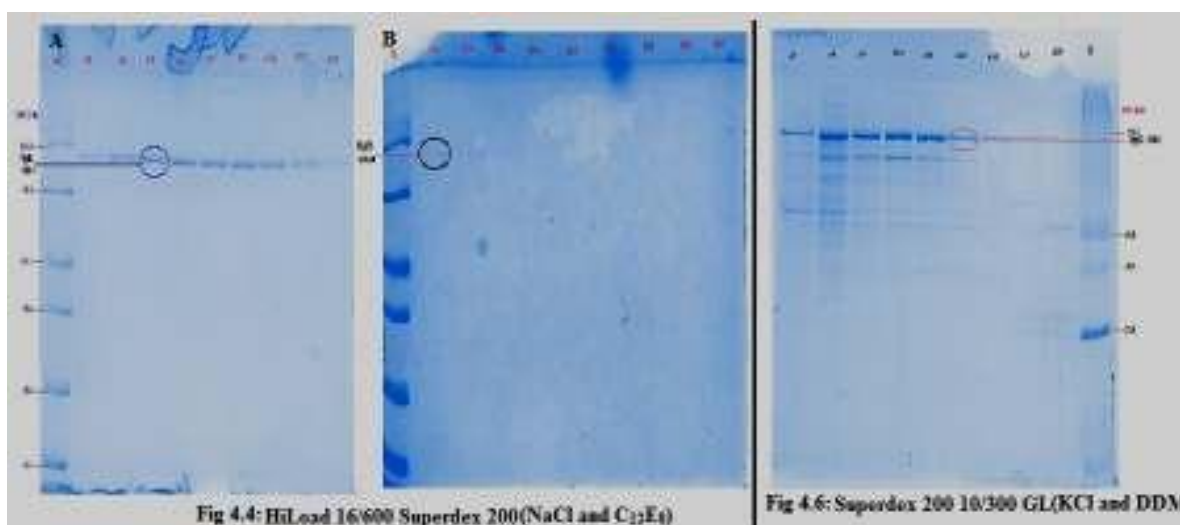
Selection of appropriate detergent for membrane protein solubilization and purification step is very important to avoid protein loss and inactivation of protein. To select detergent for MgtB protein purification, Agilent affinity system with Tosoh column TSKgel G3000SW was used. In this method, two different detergents $C_{12}E_8$ and DDM were used with same salt NaCl in separation buffer to compare the purity of MgtB protein. From the result, it was observed that the MgtB protein is more solubilized in 100 mM NaCl with detergent 0.45 mM $C_{12}E_8$ rather than 400 mM NaCl with detergent 1 mM DDM (figure 4.8 and 4.10) because the gel picture from 400 mM NaCl with detergent 1 mM DDM showed some impurities or degradation of protein (Figure 4.10).

Fig 4.8: TSKgel G3000SW (NaCl and $C_{12}E_8$)   Fig 4.10: TSKgel G3000SW (NaCl and DDM)
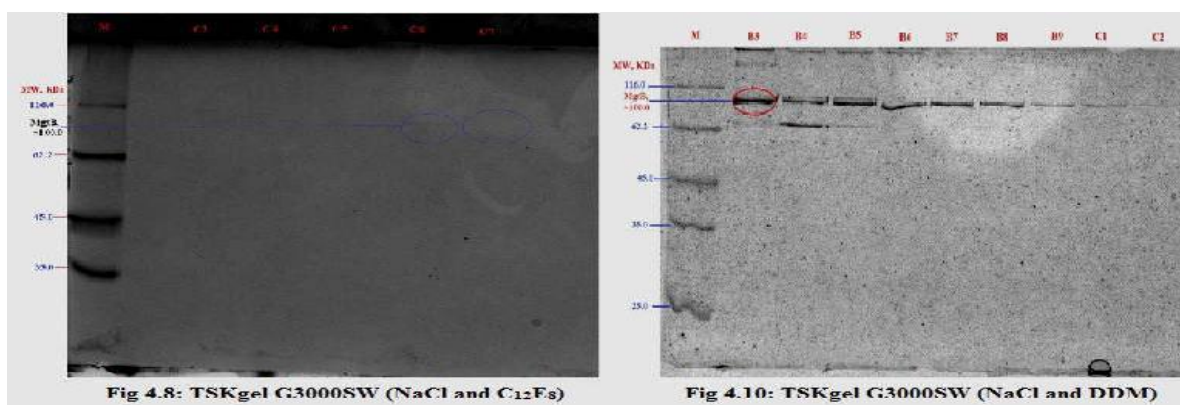
5.5 MgtB protein determination by Bradford assay

Measurement of protein concentration of MgtB in a sample solution is ardently necessary prior to crystallization. Several methods have already been developed to determine the quantitative estimation of the total protein in a sample. Among those, Bradford assay is one of the simplest and most sensitive spectroscopic analytical methods to quantify the concentration of protein. In assay, the dye Coomassie Brilliant Blue-G250 specifically binds to the side chain of Tyrosine in protein molecules. In present study, different known concentrations of Bovine Serum Albumin (BSA) was used to make a standard curve using Bradford assay to measure the concentration of MgtB protein. Though there is an outsized scale of curvature over a broad range of BSA protein concentrations but to get a linear regression in calibration or standard curve only a narrow range of BSA protein concentrations were used in the present experiment [48]. The binding of dye to BSA proteins is absorbed at wavelength 595 nm that was considered in the experiment. The absorbance at 595 nm of dye-BSA protein complex is proportional to the concentration of BSA

protein that showed a linear relationship in Bradford curve (figure 3.6). In the graph, some of data showed imprecise data points that have not fit on the line of the curve and pushed the curve nonlinear. Without minimizing this problem, this calibration graph might give a large error that will reduce the accuracy of the standard curve as well as the value of linear equation. To avoid this only accurate data points were considered to make the linear curve and it showed a good value of regression linear (R^2) 0.983 which is near to the regression linear value 1.0 that mean the data points in linear curve were considerably fit to the trend line.

5.6 Activity assay of MgtB protein

It is considered that Magnesium (Mg^{2+}) is transported from periplasmic side to cytoplasmic side by MgtB. In Mg^{2+} pump both ATP and MgtB need Mg^{2+}. By using Mg^{2+}, ATP is phosphorylated and gives the energy to activate the MgtB transporter to transport Mg^{2+} from periplasm to cytoplasm in cell membrane. It needs to decouple the activity and check whether MgtB transport Mg^{2+}, it became obligatory to reconstitute MgtB protein into liposome. The released phosphate group (Pi) from ATP is absorbed at wavelength 690 nm, but it was not performed in this experiment because of heavy precipitation that was observed in some wells. The activity assay result of MgtB protein was conducted by eye visualization method because of precipitation at the bottom side of some wells. The blue coloration in some wells indicates the phosphate group (pi) is hydrolysis from ATP by MgtB. After these observations it was concluded that MgtB protein might be active but further study is required to know the specific activity of MgtB.

5.7 Crystallography plate observation

Crystallization of a protein represents a detailed complete structure of its large number of molecules. During crystal formation protein molecules bind each other by hydrogen bonds through inner water molecules. To get a membrane protein crystal is still very complicated [49]. In the present study, experiment was conducted to obtain crystal of bacterial membrane protein MgtB from *Salmonella typhimurium*. Different types of commercial screens were used to screen for the protein MgtB crystals condition as that described in section 3.4.1 by using both hanging-drop and sitting-drop vapor diffusion methods. Each well was inspected by under stereo light microscope. The picture (Figure 4.11) was taken from the specific wells where crystals appeared (section 4.6). But crystals were confirmed to be false positive results. The

wells that showed clear drop after mixing MgtB protein sample and buffer solution from commercial screen refers as false negative result and most of the wells from crystallography plate showed false negative result in this experiment. Though constant temperature (12 °C) was maintained during crystal growth, it was not possible to maintain the same temperature during crystal plate observation. In some wells of crystal growing plate air bubbles were observed (Figure 4.11, C). The bubble could be formed at the time of mixing protein sample with commercial buffer screen onto the glass cover slip. In crystal growing plate, only three wells showed the crystal but, turned out to be false positive by checking with empty cryo-loop mounted on a pin. When tried to fish the crystals, but the crystals cracked. This might happened because the initial crystals hit were produced from the salt of the buffers and not by MgtB. Besides sometimes pieces of glass from glass cover slip or dust might be misinterpreted as crystals which was also considered as false positive in this experiment [49]. Since in this present experiment, no crystal from MgtB protein was observed and only false positives like salt crystals were observed, they were not proceed for further X-ray diffraction experiment.

6. Conclusion

This thesis describes an attempt to optimize the purification and characterization of recombinant MgtB protein. The experimental result gives an idea about the buffer, pH and salt concentration that MgtB was more stable, which is 10 mM Tris-HCl pH 7.6 and 100 mM NaCl concentration. Even though it was observed that the lipid bilayers of MgtB protein was adequately solubilized by detergent DDM, the detergent $C_{12}E_8$ showed better analytical result during purification. In this experiment, no positive crystals were observed from MgtB crystal setup. This could be because of protein instability and aggregation of protein-detergent complex during crystallization. Even though, MgtB showed some crystals in some conditions they turned to be false positive. The reason of getting insufficient purified MgtB protein after every time MgtB purification, it was not possible to set up more crystal plate by using other commercial screens.

7. Future perspectives

Today, it is still considered a challenge to express, purify, crystallize and analyze the membrane protein like MgtB. To avoid MgtB protein degradation, buffer compositions should be optimized further. In buffer composition, changing of protease inhibitor could give better result to avoid protein degradation. Western-Blot and Peptide-Mass-Fingerprinting techniques should be considered to verify for certain the near lower protein band is also MgtB band that found in SDS-gel picture. Mass spectrometry analysis is also necessary for the degraded protein band to find out where the cleavage occurs. Besides, in Ni-column stripping buffer, using Citrate instead of EDTA that can be used to inactive metalloprotease and avoid the strip of Nickel resin, could show better MgtB purification result by grabbing accessible metals and sequester them from metalloprotease. In this experiment Ni-NTA column was set up with Peristaltic pump (Minipuls 3, Gilson) with long tubing system which may led the problem to mix one fraction to next. To avoid this problem, Ni-NTA column should be set up with AKTA purifier to elute MgtB from Ni-column and collect all fractions precisely. Temperature optimization could improve the protein stability. Though MgtB is temperature sensitive, it could be important to maintain an optimum temperature during MgtB purification and crystallization set up. To avoid aggregation of protein-detergent complex empirical stability screening is necessary. This empirical stability screening will help to choose the appropriate detergent with optimal concentration for MgtB protein solubilization and purification in further studies. Gel

filtration technique can be used for assessing the suitability of different detergents for MgtB crystallization. Since, in this experiment two different detergents were used for MgtB solubilization and purification step, column-based approaches for detergent exchange can give more efficient result instead of dialysis of protein sample. Different assay tests are also necessary to confirm the activity and function of MgtB in magnesium transporting pump. Reconstitution of MgtB with artificial lipid bilayer is also necessary prior to check it in functional assay. To achieve a crystal structure of MgtB, several factors and experimental moderations are needed to be considered, with additional experiment that include lipidation and biochemical characterization of MgtB are also suggested in future studies.

References

1. Li, L., et al., *A novel family of magnesium transport genes in Arabidopsis.* Plant Cell, 2001. **13**(12): p. 2761-75.

2. Moncrief, M.B. and M.E. Maguire, *Magnesium transport in prokaryotes.* J Biol Inorg Chem, 1999. **4**(5): p. 523-7.

3. Agus, Z.S. and M. Morad, *Modulation of cardiac ion channels by magnesium.* Annu Rev Physiol, 1991. **53**: p. 299-307.

4. Altura, B.M., *Basic biochemistry and physiology of magnesium: a brief review.* Magnes Trace Elem, 1991. **10**(2-4): p. 167-71.

5. Flatman, P.W., *Mechanisms of magnesium transport.* Annu Rev Physiol, 1991. **53**: p. 259-71.

6. Maguire, M.E., *MgtA and MgtB: prokaryotic P-type ATPases that mediate Mg2+ influx.* J Bioenerg Biomembr, 1992. **24**(3): p. 319-28.

7. Matsuda, H., *Magnesium gating of the inwardly rectifying K+ channel.* Annu Rev Physiol, 1991. **53**: p. 289-98.

8. Romani, A., C. Marfella, and A. Scarpa, *Cell magnesium transport and homeostasis: role of intracellular compartments.* Miner Electrolyte Metab, 1993. **19**(4-5): p. 282-9.

9. Tao, T., et al., *Magnesium transport in Salmonella typhimurium: mgtA encodes a P-type ATPase and is regulated by Mg2+ in a manner similar to that of the mgtB P-type ATPase.* J Bacteriol, 1995. **177**(10): p. 2654-62.

10. Grubbs, R.D. and M.E. Maguire, *Magnesium as a regulatory cation: criteria and evaluation.* Magnesium, 1987. **6**(3): p. 113-27.

11. Hmiel, S.P., et al., *Magnesium transport in Salmonella typhimurium: genetic characterization and cloning of three magnesium transport loci.* J Bacteriol, 1989. **171**(9): p. 4742-51.

12. Snavely, M.D., et al., *Magnesium transport in Salmonella typhimurium: 28Mg2+ transport by the CorA, MgtA, and MgtB systems.* J Bacteriol, 1989. **171**(9): p. 4761-6.

13. Snavely, M.D., et al., *Magnesium transport in Salmonella typhimurium. Regulation of mgtA and mgtB expression.* J Biol Chem, 1991. **266**(2): p. 824-9.

14. Snavely, M.D., C.G. Miller, and M.E. Maguire, *The mgtB Mg2+ transport locus of Salmonella typhimurium encodes a P-type ATPase.* J Biol Chem, 1991. **266**(2): p. 815-23.

15. Smith, R.L., L.J. Thompson, and M.E. Maguire, *Cloning and characterization of MgtE, a putative new class of Mg2+ transporter from Bacillus firmus OF4.* J Bacteriol, 1995. **177**(5): p. 1233-8.

16. Hmiel, S.P., et al., *Magnesium transport in Salmonella typhimurium: characterization of magnesium influx and cloning of a transport gene.* J Bacteriol, 1986. **168**(3): p. 1444-50.

17. Kuhlbrandt, W., *Biology, structure and mechanism of P-type ATPases.* Nat Rev Mol Cell Biol, 2004. **5**(4): p. 282-95.

18. Smith, D.L., T. Tao, and M.E. Maguire, *Membrane topology of a P-type ATPase. The MgtB magnesium transport protein of Salmonella typhimurium.* J Biol Chem, 1993. **268**(30): p. 22469-79.

19. Bublitz, M., J.P. Morth, and P. Nissen, *P-type ATPases at a glance.* J Cell Sci, 2011. **124**(Pt 15): p. 2515-9.

20. Skou, J.C., *The influence of some cations on an adenosine triphosphatase from peripheral nerves.* J Am Soc Nephrol, 1998. **9**(11): p. 2170-7.

21. Palmgren, M.G. and K.B. Axelsen, *Evolution of P-type ATPases.* Biochim Biophys Acta, 1998. **1365**(1-2): p. 37-45.

22. Buurman, E.T., K.T. Kim, and W. Epstein, *Genetic evidence for two sequentially occupied K+ binding sites in the Kdp transport ATPase.* J Biol Chem, 1995. **270**(12): p. 6678-85.

23. Lenoir, G., P. Williamson, and J.C. Holthuis, *On the origin of lipid asymmetry: the flip side of ion transport.* Curr Opin Chem Biol, 2007. **11**(6): p. 654-61.

24. Palmgren, M.G. and P. Nissen, *P-type ATPases.* Annu Rev Biophys, 2011. **40**: p. 243-66.

25. Scarborough, G.A., *Molecular mechanism of the P-type ATPases.* J Bioenerg Biomembr, 2002. **34**(4): p. 235-50.

26. Bertucci, A., et al., *Symbiosis-dependent gene expression in coral-dinoflagellate association: cloning and characterization of a P-type H+-ATPase gene.* Proc Biol Sci, 2010. **277**(1678): p. 87-95.

27. Apell, H.J., *How do P-type ATPases transport ions?* Bioelectrochemistry, 2004. **63**(1-2): p. 149-56.

28. Fagan, M.J. and M.H. Saier, Jr., *P-type ATPases of eukaryotes and bacteria: sequence analyses and construction of phylogenetic trees.* J Mol Evol, 1994. **38**(1): p. 57-99.

29. Serrano, R., *Structure and function of proton translocating ATPase in plasma membranes of plants and fungi.* Biochimica et Biophysica Acta (BBA) - Reviews on Biomembranes, 1988. **947**(1): p. 1-28.

30. Kyte, J. and R.F. Doolittle, *A simple method for displaying the hydropathic character of a protein.* J Mol Biol, 1982. **157**(1): p. 105-32.

31. Monsieurs, P., et al., *Comparison of the PhoPQ regulon in Escherichia coli and Salmonella typhimurium.* J Mol Evol, 2005. **60**(4): p. 462-74.

32. Gunzel, D., et al., *The MgtC virulence factor of Salmonella enterica serovar Typhimurium activates Na(+),K(+)-ATPase.* J Bacteriol, 2006. **188**(15): p. 5586-94.

33. Lee, E.J. and E.A. Groisman, *An antisense RNA that governs the expression kinetics of a multifunctional virulence gene.* Mol Microbiol, 2010. **76**(4): p. 1020-33.

34. Lee, E.J. and E.A. Groisman, *Tandem attenuators control expression of the Salmonella mgtCBR virulence operon.* Mol Microbiol, 2012. **86**(1): p. 212-24.

35. Lesk, A.M., *Introduction to protein architecture : the structural biology of proteins.* 2001, Oxford ; New York: Oxford University Press. xii, 347 p.

36. Wlodawer, A., et al., *Protein crystallography for non-crystallographers, or how to get the best (but not more) from published macromolecular structures.* FEBS J, 2008. **275**(1): p. 1-21.

37. Evangelopous, D. and J.D. Guzman *The Art of Protein Crystallization.* Bench philosophy (27): Protein crystallization guide, 2010. **6-2010**, 74-76.

38. Gale, R., *Crystallography Made Crystal Clear, Third Edition.* Academic Press. 1993.

39. McCormick, B.A., et al., *Transepithelial signaling to neutrophils by salmonellae: a novel virulence mechanism for gastroenteritis.* Infect Immun, 1995. **63**(6): p. 2302-9.

40. Everest, P., et al., *Evaluation of Salmonella typhimurium mutants in a model of experimental gastroenteritis.* Infect Immun, 1999. **67**(6): p. 2815-21.

41. Moncrief, M.B. and M.E. Maguire, *Magnesium and the role of MgtC in growth of Salmonella typhimurium.* Infect Immun, 1998. **66**(8): p. 3802-9.

42. Berg JM, T.J., Stryer L., *Biochemistry.* Section 4.1, The Purification of Proteins Is an Essential First Step in Understanding Their Function. Vol. 5th edition. 2002, New York: W H Freeman.

43. Smits, S.H., et al., *Coenzyme- and His-tag-induced crystallization of octopine dehydrogenase.* Acta Crystallogr Sect F Struct Biol Cryst Commun, 2008. **64**(Pt 9): p. 836-9.

44. Kapust, R.B., et al., *The P1' specificity of tobacco etch virus protease.* Biochem Biophys Res Commun, 2002. **294**(5): p. 949-55.

45. Nallamsetty, S., et al., *Efficient site-specific processing of fusion proteins by tobacco vein mottling virus protease in vivo and in vitro.* Protein Expr Purif, 2004. **38**(1): p. 108-15.

46. Bolanos-Garcia, V.M. and O.R. Davies, *Structural analysis and classification of native proteins from E. coli commonly co-purified by immobilised metal affinity chromatography.* Biochim Biophys Acta, 2006. **1760**(9): p. 1304-13.

47. Hochuli, E., et al., *Genetic Approach to Facilitate Purification of Recombinant Proteins with a Novel Metal Chelate Adsorbent.* Nature Biotechnology, 1988. **6**(11): p. 1321-1325.

48. Ernst, O. and T. Zor, *Linearization of the bradford protein assay.* J Vis Exp, 2010(38).

49. *Methods and Results in Crystallization of Membrane Proteins*, ed. S. Iwata. International Unversity Line.

Appendix

Preparation of Cell Lysis Buffer (1)

Chemical name	Concentration
Tris-HCl pH 7.6	50 mM
NaCl	50 mM
MgCl$_2$.6H$_2$O	1 mM
PMSF (Phenyl methyl sulfonyl fluoride)	1 mM
BME (2 MercaptoEtOH)	5 mM
Glycerol	10%
ATP	1 μl

Preparation of Cell Lysis Buffer (2)

Chemical name	Concentration
Tris-HCl pH 7.6	50 mM
NaCl/KCl	200 mM
MgCl$_2$.6H$_2$O	1 mM
PMSF (Phenyl methyl sulfonyl fluoride)	1 mM
BME (2 MercaptoEtOH)	5 mM
Glycerol	10%

Preparation of Membrane resuspension buffer (1)

Chemical name	Concentration
Tris-HCl pH 7.6	50 mM
NaCl	50 mM
$MgCl_2.6H_2O$	1 mM
BME (2 MercaptoEtOH)	5 mM
Glycerol	10%
ATP	1 µM

Preparation of Membrane resuspension buffer (2)

Chemical name	Concentration
Tris-HCl pH 7.6	50 mM
NaCl/KCl	200 mM
$MgCl_2.6H_2O$	1 mM
BME (2 MercaptoEtOH)	5 mM
Glycerol	10%

Preparation of Buffer A (1)

Chemical name	Concentration
Tris-HCl pH 7.6	50 mM
NaCl	50 mM
BME (2 MercaptoEtOH)	5 mM
Glycerol	10%
Imidazole	20 mM
$MgCl_2.6H_2O$	1 mM
DDM	1 mM
ATP	1 µM

Preparation of Buffer A (2)

Chemical name	Concentration
Tris-HCl pH 7.6	50 mM
NaCl/KCl	200 mM
BME (2 MercaptoEtOH)	5 mM
Glycerol	10%
Imidazole	20 mM
$MgCl_2.6H_2O$	1 mM
DDM	1 mM

Preparation of Buffer B (1)

Chemical name	Concentration
Tris-HCl pH 7.6	50 mM
NaCl	50 mM
BME (2 MercaptoEtOH)	5 mM
Glycerol	10%
Imidazole	500 mM
MgCl$_2$.6H$_2$O	1 mM
DDM	1 mM
ATP	1 µM

Preparation of Buffer B (2)

Chemical name	Concentration
Tris-HCl pH 7.6	50 mM
NaCl/KCl	200 mM
BME (2 MercaptoEtOH)	5 mM
Glycerol	10%
Imidazole	500 mM
MgCl$_2$.6H$_2$O	1 mM
DDM	1 mM

Preparation of Gel filtration Buffer (1)

Chemical name	Concentration
Tris-HCl pH 7.6	10 mM
NaCl	100 mM
Glycerol	10%
DTT	1 mM
$C_{12}E_8$	0.45 mM
ATP	1 μM

Preparation of Gel filtration Buffer (2)

Chemical name	Concentration
Tris-HCl pH 7.6	20 mM
NaCl/KCl	100 mM
Glycerol	10%
DTT	2.5 mM
DDM	1 mM

Preparation of Dialysis buffer

Chemical name	Concentration
Tris-HCl pH 7.6	50mM
NaCl	50mM
BME (2 MercaptoEtOH)	5mM
Glycerol	10%
$MgCl_2.6H_2O$	1mM
ATP	$1\mu M$

MgtB sample preparation for Gel Electrophoresis (SDS-PAGE)

	Load	Run Through	Wash	Imidazole Concentration (mixture of buffer A and B)										Marker (M)
				100mM			300mM			500mM				
				1	2	3	4	5	6	7	8	9	10	6µl
MgtB	5µl	5µl	5µl	10µl	10µl	10µl	10µl	10µl	10µl	10µl	10µl	10µl	10µl	
Loading Buffer	5µl	5µl	5µl	5µl	5µl	5µl	5µl	5µl	5µl	5µl	5µl	5µl	5µl	
MiliQ water	5µl	5µl	5µl											